Polymer Testing 93 (2021) 106925

Contents lists available at ScienceDirect

Polymer Testing

journal homepage: http://www.elsevier.com/locate/polytest

The mechanical testing and performance analysis of polymer-fibre composites prepared through the additive manufacturing

Vigneshwaran Shanmugam [a,***], Deepak Joel Johnson Rajendran [b], Karthik Babu [c], Sundarakannan Rajendran [a], Arumugaprabu Veerasimman [a], Uthayakumar Marimuthu [a], Sunpreet Singh [d], Oisik Das [h,*], Rasoul Esmaeely Neisiany [f,**], Mikael S. Hedenqvist [e], Filippo Berto [g], Seeram Ramakrishna [d,****]

[a] Faculty of Mechanical Engineering, Kalasalingam Academy of Research and Education, Krishnankoil, 626 126, India
[b] Faculty of Mechanical Engineering, Saveetha School of Engineering, Saveetha Institute of Medical and Technical Sciences, Thandalam, Chennai, 602 105, India
[c] Center for Polymer Composites and Natural Fibre Research, Tamil Nadu, 625005, India
[d] Department of Mechanical Engineering, National University of Singapore, 117575, Singapore
[e] Department of Fibre and Polymer Technology, School of Engineering Sciences in Chemistry, Biotechnology and Health, KTH Royal Institute of Technology, Stockholm, 100 44, Sweden
[f] Department of Materials and Polymer Engineering, Faculty of Engineering, Hakim Sabzevari University, Sabzevar, 9617976487, Iran
[g] Department of Mechanical and Industrial Engineering, Norwegian University of Science and Technology NTNU, S.P. Andersens Veg 3, Trondheim, 7031, Norway
[h] Structural and Fire Engineering Division, Department of Civil, Environmental and Natural Resources Engineering, Luleå University of Technology, Luleå, SE-97187, Sweden

ARTICLE INFO

Keywords:
Additive manufacturing
3D printing
Fused deposition modelling
Natural fibre composites
Mechanical properties

ABSTRACT

The development of fibre composites in recent years has been remarkably strong, owing to their high performance and durability. Various advancements in fibre composites are emerging because of their increased use in a myriad of applications. One of the popular processing methods is additive manufacturing (AM), however, polymer-fibre composites manufactured through AM have a significantly lower strength compared to the conventional manufacturing processes, for instance, injection moulding. This article is a comprehensive review of the mechanical testing and performance analysis of polymer-fibre composites fabricated through AM, in particular fused deposition modelling (FDM). The review highlights the effect of the various processing parameters, involved in the FDM of polymer-fibre composites, on the observed mechanical properties. In addition, the thermal properties of FDM based fibre composites are also briefly reviewed. Overall, the review article has been structured to provide an impetus for researchers in the concerned engineering domain to gain an insight into the mechanical properties of fibre-reinforced polymeric composites manufactured through AM.

1. Introduction

Additive manufacturing (AM) is a novel manufacturing process, generally known as 3D printing, which has been utilised for the processing of metals and polymers [1–3]. Products produced through AM are developed by adding layer-by-layer of material, whereas, in traditional methods, products are developed through subtractive manufacturing methods [4–6]. The low cost and versatility in developing complex designs have increased the utilisation of AM in modern applications [7] such as product development in the automotive industry, aerospace/biomedical applications, the development of arts and designs, architecture, etc. [8,9]. The development of AM has evolved vigorously after 2013 owing to their increased use in the aforementioned applications, and the number of academic publications has

* Corresponding author.
** Corresponding author.
*** Corresponding author.
**** Corresponding author.
E-mail addresses: s.vigneshwaren@gmail.com (V. Shanmugam), uthaykumar@gmail.com (U. Marimuthu), Odas566@aucklanduni.ac.nz, oisik.das@ltu.se (O. Das), r.esmaeely@hsu.ac.ir (R.E. Neisiany), seeram@nus.edu.sg (S. Ramakrishna).

https://doi.org/10.1016/j.polymertesting.2020.106925
Received 20 July 2020; Received in revised form 9 September 2020; Accepted 20 October 2020
Available online 23 October 2020

increased markedly over the last five years [10]. At present, AM technology is widely used in aerospace, electronics, and biomedical applications [11–13]. AM is a flexible manufacturing process that develops the product directly from the design file, thereby reducing product lead time and material waste, and a complex design can also be developed economically [14]. However, there are few drawbacks in the AM process, such as slow mass production and limited material use, which restrict it in a number of applications. In particular, AM has very selective material applications [15–17], since the additive manufactured materials are largely found only as a prototype model [18]. In this regard, the multiple printing head technique has been developed where composite material can be created using controlled material combinations and properties [11]. The development of fibre composites is a more challenging approach for the AM process. Several aspects need to be considered for the development of fibre composites, including fibre/-matrix weight percentage, fibre/matrix interactions, fibre length, fibre orientation, and fibre type [19,20]. Five main AM fabrication techniques for polymeric materials are stereolithography (SLA), laminated object manufacturing (LOM), fused deposition modelling (FDM), selective laser sintering (SLS), and multi-jet fusion (MJF) [21,22].

Polymers are the most widely used materials in many applications due to their high performance, ease of production, and low cost. In AM, polymers are used in a variety of forms, such as reactive, liquid, and thermoplastic melts [23]. Filled polymers have been developed in recent years through the AM process, and commonly used fillers are carbon fibres, carbon nanotubes, nanoparticles, nanoparticles/nanofillers, and various synthetic fibres [24]. The addition of these fillers improves the mechanical properties of the composites manufactured through AM [25]. The development of fibre/filler reinforced polymers provides a synergistic effect in terms of improved performance and polymer characteristics [26,27]. This could also benefit other AM processes in the development of fibre/filled composites. The addition of fibre to the material could reduce the bending and warping during deposition [20]. Some changes need to be made to the AM process for the development of filled polymers. Short and discontinuous fibres are preferred in AM due to the complexity linked to the use of long and continuous fibres. Through AM, fibre composites can be produced cost-effectively. However, AM of fibre composites is still at its infancy where some critical issues need to be resolved.

Fused deposition modelling (FDM) is one of the versatile additive manufacturing techniques (AM) used for 3D printing of polymers and their composites. In this process, successive layers of material are deposited using a computer-machine interface to create a 3D object. FDM-based polymer research has increased in recent years due to its flexibility in the production of polymer and fibre-based composites. FDM-based polymers have the potential to be used in different applications, Fig. 1 shows the scope of FDM based polymers in various applications.

Relatively few review articles are available on FDM-based polymer [28–30] and the real interest in 3D printing of polymers in the contemporary research is to achieve enhanced strength. The available review articles advocate the need for the development of 3D printed polymers and composites. However, there is a dearth of a dedicated and comprehensive review article explaining the mechanical and thermal properties of FDM-based reinforced fibre composites. In this light, the current article discusses the state of the art of FDM-based fibre composite performance by considering various constraints and challenges. The implications of layer bonding, fibre matrix characteristics, fibre matrix interface and FDM printing variables on the mechanical and thermal performance of FDM fibre composites have been critically reviewed and discussed to meet the research needs of developing high-strength fibre composites through FDM-AM.

1.1. Steps involved in AM

AM involves a series of processes, from design development to final product manufacturing, which varies depending on the type of manufacturing method used [31]. These primary processes are common and remain the same for any type of manufacturing, whether it is a prototype or a functional product. The steps involved in the AM process are shown in Fig. 2.

Fig. 1. Scope of FDM based polymers/composites in various applications.

1.1.1. Production of the digital model

Initially, the digital model of the part is designed through CAD software in this process. Reverse engineering and 3D scanning are also used to develop a digital model [32].

1.1.2. STL conversion

Secondly, the digital model is converted into the Standard Triangle Language (.STL) or Standard Tessellation Language file [33–36]. The. STL file stores information on model surface geometry [37–40].

1.1.3. Slicing

After conversion, the.STL file is fed to the slicer program [41]. Slicing is crucial in determining the quality of the printed parts [42]. The slicer is used to generate G-codes based on the information in the.STL file [43–45]. The G-code produced is similar to the CNC machine codes and it defines the movement of the extruder and the platform direction during printing [46–48].

1.1.4. Printing

After converting the.STL file to G-codes, the 3D printer is ready to print the design. The printing varies depending on the type of AM process involved. In FDM, the nozzle moves and deposits the molten filament layer by layer, based on the G-code instructions [48]. The movement of the extruding nozzle, the amount of the material extruded, and the extrusion time are controlled by the G-code. When the entire

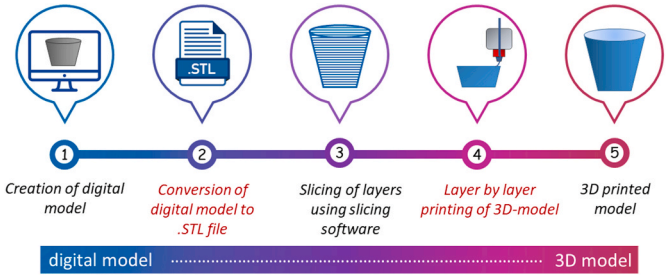

Fig. 2. Steps in AM – digital model to 3D model.

model printing is completed, some post-processing needs to be done to achieve a proper product finish [49]. Post-processing methods vary according to the material and manufacturing methods used [50,51].

2. AM of fibre-reinforced polymers

The strength of polymer composites can be significantly improved through fibre reinforcement. Fibre-reinforced polymers manufactured using AM techniques could have a significant impact on AM of polymers. Fibre matrix interactions and void formation are the two important considerations to be addressed in AM of fibre composites. Various techniques such as FDM, LOM, SLS, and SLA are involved in AM of fibre composites. Compared to all these techniques, FDM is the most preferred method for the production of fibre composites due to its scalability, material flexibility, and precision.

2.1. Fused deposition modelling

FDM is the preferred method for the manufacturing of polymers due to a simple process, which is also more economical than other techniques. FDM is part of the material extrusion manufacturing process used to process thermoplastic polymers [52,53]. Some common thermoplastic filaments used in FDM are acrylonitrile butadiene styrene (ABS), polypropylene (PP), polylactide (PLA), polyether-ether-ketone (PEEK), and polyamides (PA), like PA6, PA12 [54]. The properties of these matrices are shown in Table 1. In FDM, the polymers are extruded and deposited in a layer by layer method for product development. Compared to other AM methods, FDM-manufactured polymers exhibit acceptable mechanical performance, good surface finish, and durability at low cost. The matrix material used in the FDM process is in the form of long wires or filament wound on to the spool. The diameter of the filament material varies from 1.75 to 2.85 mm depending on the nozzle used in the machine. The filament is initially fed into the melt head that is heated above the glass transition temperature and is converted to a plastic melt. The plastic melt is then passed to the nozzle and extruded out. The nozzle moves in XY-direction according to the design model fed to the control system. Fig. 3 shows a schematic representation of the 3D printer used in FDM. The extruded filament from the nozzle is added layer by layer over the build platform until the entire design is completed. After the completion of a single layer, the build platform moves in the Z-direction downward and the next layer is deposited and bonded to the previous layer. The distance moved by the build platform is known as the layer height, and generally, the height of the layer varies from 100 to 300 μm. A reduction in the layer height produces fine layers. At present, it is possible to print at a height as low as 25 μm.

In FDM there are different possibilities to introduce fibre reinforcement in the thermoplastic matrix [18,24,56]:

1. Direct reinforcement – here, two injectors are needed. One for injecting the matrix filament and the other for the fibre filament. These are mixed at the part after injection.
2. The fibre and the matrix are mixed before the injection.
3. Fibre and matrix are mixed before injection as a pre-impregnated filament. This method is preferred for fibre composite fabrication.

Table 1
Properties of polymer matrices used in fibre composite fabrication in FDM [10,55].

Matrix	Density (g/cm^3)	Tensile strength (MPa)	Tensile modulus (GPa)	Flexural modulus (GPa)	Printing temperature (°C)
ABS	1.04	22–37	0.998	1.9	210–250
PA	1.1	34–68	0.94	0.84	235–260
PLA	1.25	37–46	2.02	2.39	190–210
PEEK	1.3	48–265	3.5–3.9	3.7–4	360–450
PP	0.92	20–40	1.1–1.6	1.2–1.6	230–260

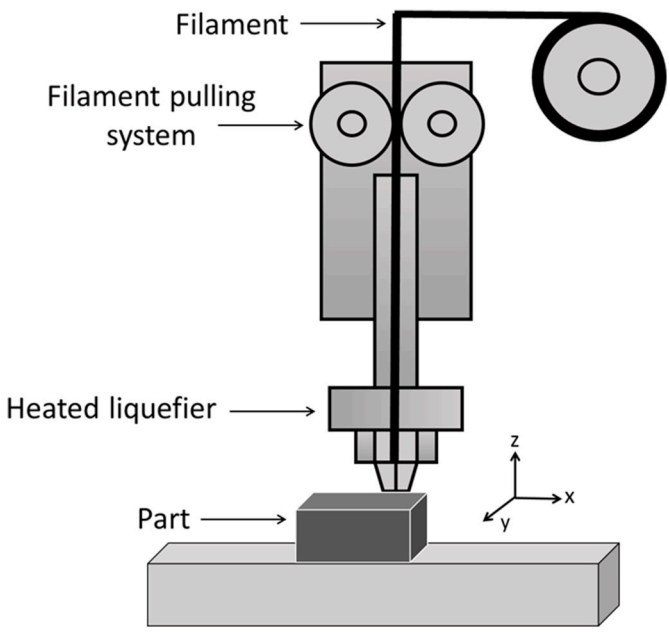

Fig. 3. 3D printer schematic representation.

Research on printing variables in terms of mechanical properties is increasing to develop high strength 3D printing models. In FDM, overhanging models are supported by structures that are water-soluble or can be dissolved. Melt temperature, thermal conductivity, heat capacity, cooling rate, viscosity, raster width, raster angle, printing orientation, air gap, and layer height are some important variables in FDM-3D polymer printing [57]. The bonding of each layer is crucial to the development of high strength polymers through FDM. Variation in the raster angle changes the mechanical properties of the composite since it alters the load transfer within layers [58]. Variation in print orientation may induce anisotropic properties in the printed part [59]. Mohamed et al. [60] reported that the process parameters involved in the product/prototype development through FDM account for the quality and mechanical performance. The control factors to be considered during the processing of AM are shown in Fig. 4(a) and the factors affecting the 3D printed part quality and mechanical performance are shown in Fig. 4 (b).

Anitha et al. [61] reported that the layer thickness has a significant influence on the surface roughness of the fabricated part, where 50% of layer thickness contributed to affecting the surface roughness of the FDM printed component. A reduction in layer thickness allows for a lower surface roughness [62–64]. Since FDM based 3D printing is a relatively new technique, it is essential to compare the strength of parts produced by conventional manufacturing processes such as injection moulding, compression moulding and so on. In this view, Carneiro et al. [65] reported that the FDM printed PP samples showed lower tensile strength and modulus compared to the compression moulded samples, although adequate tensile strength and modulus of the printed products were achieved by controlling the FDM process variables. The bonding between the successive layers and voids is a major concern in the FDM parts and these factors govern the mechanical strength of the parts. Bellehumeur et al. [66] quantitatively assessed the bonding quality of the printed material by analysing the degree of wetting or the size of the neck formed between successive filaments. The results indicated that the extrusion temperature had a significant impact on the neck growth of the bonding region compared to the environment temperature. Riddick et al. [67] used scanning electron microscope (SEM) images to investigate the effects of build directions (horizontal, side, and vertical directions) and raster orientation (±45°, 0°, 90°, and 0°/90°) on the tensile properties and failure mechanism of FDM printed ABS material.

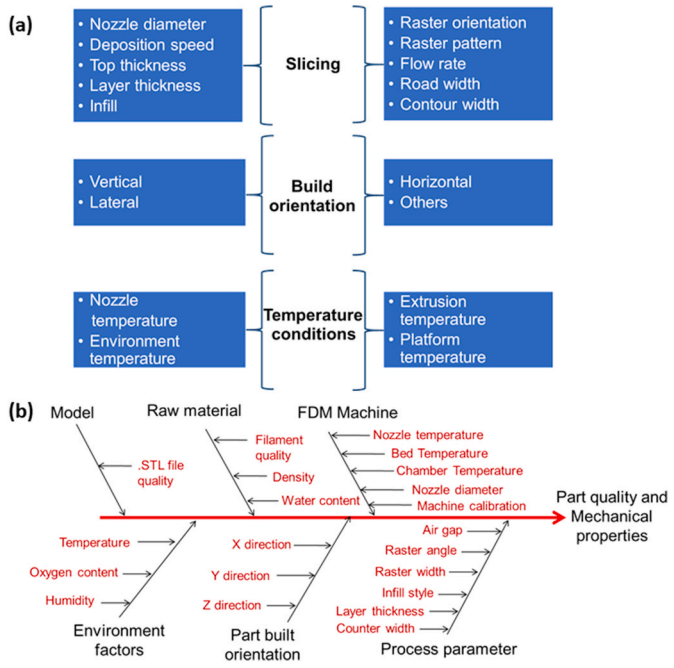

Fig. 4. (a) FDM process parameters, (b) Factors affecting FDM part quality and mechanical performance.

It has been observed that the raster orientation and the build direction have an impact on the tensile strength, modulus, and the elongation-at-break of the ABS material. The maximum tensile strength of 34 MPa was recorded for the sample printed at 0° raster orientation with side build direction and the lowest was recorded on the 90° raster orientation with vertical build direction. The maximum elongation at break was 1.5% for the sample printed at a raster orientation of 45° with horizontal build direction. Therefore, optimisation of printing parameters is necessary to improve the printing quality [68,69]. Tekinalp et al. [70] found high amounts of triangle-shaped voids on the ABS/carbon fibre composite fabricated through FDM, formed mainly because of the gaps between the beads deposited during printing. Kalita et al. [71] developed PP composite with tricalcium phosphate (TCP) ceramic reinforcement at varying volume % of porosity (36%, 48%, and 52%) through FDM. Porosity is the function of FDM printing variables as well as the properties of the polymer and reinforcing material [72]. Air pores in the FDM parts can be reduced by printing at a high nozzle temperature due to better material fluidity at high nozzle temperature [73].

2.2. Bond formation between layers in FDM

In AM, bonding between the layers is a crucial factor for governing the mechanical strength of the part or of the composite. During printing, the bond formation between the layers does not involve any externally applied force/pressure, bonding occurs because of the high temperature in the newly deposited layer [74]. Several researchers have reported the importance of inter-layer bonding in FDM, which occurs through local "welding" of adjacent layers. The final 3D printed parts' meso-structural characteristics and the degree of inter-layer bonding significantly affect the strength since, under loading, the weakly bonded layer fails first. The mesostructure of the 3D printed part describes the growth of the neck between the layer lines, as well as the formation of bonds and voids between the layers. Variation in the bonding and formation of voids creates inhomogeneity in the printed parts that directly affect the mechanical performance of the part [75,76]. It is important to understand the relationship between process parameters and part performance to optimise the quality of 3D printed components [25]. However, the number of investigations on inter-layer bonding in FDM is rather limited. Developing models for predicting and analysing layer bonding and for evaluating their impact on mechanical performance and fracture resistance would improve knowledge of 3D printed part performance. In FDM, printing speed and complexity of temperature variation are critical, making it difficult to achieve consistency in bonding strength and molecular diffusion [77]. Aliheidari et al. [76] investigated the inter-layer bonding characteristics of ABS material regarding the softening temperature, bed temperature, layer height, and layer width. Improvement in bonding was noted at increased layer width, owing to the increase in the area of adhesion. This reduced the formation of voids since the total number of layers in the crack plane decreased; correspondingly the mechanical performance was also increased.

The interlayer bonding strength of FDM printed polymer is the function of FDM printing parameters [78] such as temperature, viscosity, and surface energy of the thermoplastic melt [79,80]. The inter-layer bond formation in the ABS polymer was analysed by Bellehumeur et al. [66] through the Newtonian polymer sintering model developed by Pokluda et al. [81]. Bond formation between adjacent layers begins with the growth of a neck. Sun et al. [82] reported that the mechanical performance of the part is closely related to the variation in the cooling temperature and critical sintering temperature. Fig. 5 explains the mechanism of neck formation between adjacent layers. The formation of the neck depends on the viscosity of the matrix. During the necking process, the polymer molecules in the separate layers inter-diffuse and form the bond. As the temperature decreases the matrix viscosity increases, which slowly reduces the neck formation as well as the diffusion process. This process depends on the polymer viscosity, thermal conductivity, heat capacity, and cooling rate. The layer bond can be increased at high temperature but at a significantly high temperature, polymer degradation may occur, which produces poor surface finish and dimensional inaccuracies [80]. Li et al. [83] reported that the neck growth between the adjacent beads develops when the temperature is above the critical sintering temperature. The deposited layer solidification time should be short to achieve rapid bonding, and after solidification, the part should be free of internal stress to achieve good mechanical properties [19]. Torrado et al. [84] elaborated on the importance of layer bonding on 3D printed material properties. The results exemplify the relationship between the complex viscosity and anisotropy. The anisotropic properties of the composite can be reduced by printing at a lower viscosity and a temperature above the glass transition. This would increase the layer contact area and correspondingly increase the layer bonding.

Thomas and Rodriguez [85] developed a model to predict the thermal effect at the rectangular bead interface. The model showed that parts produced at a lower cooling rate exhibit good strength. Costa et al. [86] proposed a transient heat transfer analysis model to quantify the bonding strength of FDM parts. The model was based on the melt temperature and bonding between the filaments. Rodriguez et al. [87]

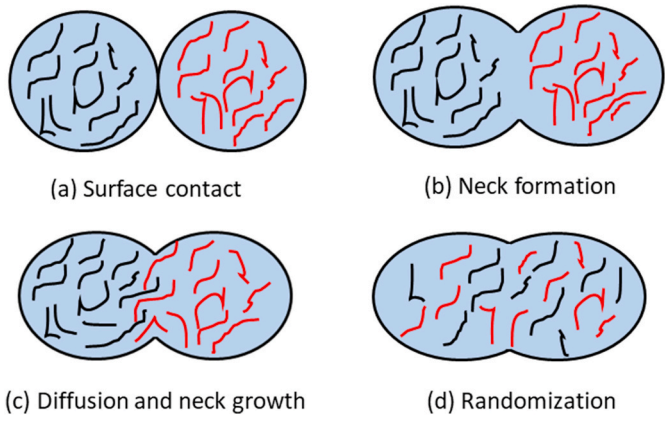

Fig. 5. Mechanism behind layer bonding.

analysed the ABS material bonding strength and reported the influence of printing parameters on the bonding strength. At low raster angle and high nozzle temperature, as well as high environment temperature, it is possible to produce well-bonded ABS parts. Aliheidari et al. [88] reported that the interfacial bonding between the layers of ABS material increases the fracture resistance of the material, and furthermore it is possible to obtain good bonding at high printing temperature. Samples printed at a nozzle temperature of 240 °C exhibited good bonding between the layers and increased fracture resistance. Young et al. [89] fabricated ABS composites with carbon fibre reinforcement through compression moulding and 3D printing. The 3D printed composite exhibited poor mechanical performance owing to inadequate layer adhesion. Compared to fibre-reinforced bio-polyethylene composite, pure bio-polyethylene exhibited poor bonding between the layers. Poor bonding was the reason behind increasing amounts of cracks and pores in the bio-polyethylene surface [90]. Levenhagen and Dadmun [91] reported that the addition of a bimodal blend to PLA reduced the anisotropic properties and also enhanced the mechanical strength of the 3D-printed PLA material.

Hart et al. [77] investigated the interlayer bonding of ABS thermoplastic material at four stages:

(1) Interface heating, enabling local polymer flow and molecular mobility;
(2) Intimate contact, or close physical association of the two adherent surfaces;
(3) Molecular diffusion across the interface; and
(4) Cooling of the interface to below the glass transition temperature.

The finding of the Hart et al. [77] emphasised the post-treatment of polymer to achieve enhanced inter-laminar toughness. Annealing techniques have been used to improve the inter-layer bonding [77] (Fig. 6). During the process of annealing, diffusion of polymer chains occurs through the layer interface, which shifts the material fracture behaviour from unstable to stable. It is reported that the interface can be healed by annealing at the lower glass transition temperature, while the higher glass transition temperature provides geometric stability in order to retain the shape of the part outside the annealing fixture. Wach et al. [92] reported that annealing in FDM printed PLA increased its crystallinity, leading to an increase of flexural stress from 11 to 17%. These results suggest the annealing of FDM printed parts as an effective technique to enhance the layer bonding, which could lead to an increase in mechanical strength.

3. Fibre orientation's influence in FDM part performance

In AM it is possible to change the fibre orientation during the fabrication of the composite by varying the layering pattern and raster orientation. Analysing the fibre orientation is important for understanding the fibre composite characteristics, however it is challenging [93] since the fibres cannot be aligned uniformly through FDM. Sporek et al. [94] studied the significance of flow-induced fibre orientation on the mechanical and thermal properties of a PP/carbon fibre composite. Morphological analysis showed a preferential fibre alignment along the printing direction. The fibre-fibre interactions, as well as fibre-matrix interaction, were found to be better in the developed composite. When the new layer was extruded over the pre-deposited layer, the pre-deposited layer surface started re-melting, which developed an interconnection between fibre in the two layers. This resulted in interconnected orientation of longitudinally- and orthogonally-oriented fibres [95]. The melt flow field influenced by the melt flow characteristics, such as the flow in the nozzle convergence and the extruded swell, may affect the orientation of the fibre, resulting in changes in the extruded polymer strength [96]. Zhang et al. [97] investigated the mechanical performance of a carbon fibre composite with curved and unidirectional fibre reinforcement. Finite element analysis was performed to understand the direction of the principal stress. The result of the investigation showed that the curved fibre placement followed the principal stress direction enhancing the mechanical properties of the carbon fibre composite since the curved fibre placement reduced the stress concentration and increased the stiffness. Safonov [98] developed an algorithm to analyse 3D printed fibre composite density and fibre reinforcement structure. The proposed method successfully identified the optimal distribution of material density and distribution of fibre orientation vectors for 2D beam, 3D cube, and 3D cantilever beam. However, the method did not use all of the shell elements commonly utilised in traditional composite structures analysis. Therefore, it is not possible to find the exact material density and fibre distribution for all 3D printed composites by this method. A modelling approach was developed by Heller et al. [99] to analyse the fibre orientation in the part developed through FDM. The model was developed based on the converging flow in the nozzle, fluid expansion caused by the extruded swell, and nozzle exit shape. Mohammadizadeh et al. [100] observed variations in the tensile strength of composite samples prepared in the same way and with the same content of fibres and explained it as being due to variations in the fibre orientation. Additionally, the authors observed that the part with the most uniform fibre orientation in the loading direction exhibited the best mechanical performance. Papon and Haque [101] investigated the fracture strength of short fibre reinforced PLA composites at varying orientation. From the experimental results, it was found that the composite with 5% carbon fibre printed at 45°/−45° orientation withstands the maximum fracture energy of 6.6 kJ/m^2. Pertuz et al. [102] fabricated a PA composite with carbon, kevlar, and glass fibre reinforcements. The composites were printed at varying orientations 0, 45, and 60°. The fibre orientation was varied by changing the layering direction. Fig. 7 shows the fibre layer orientation. The composite with 0° fibre orientation exhibited better mechanical performance than the 45° and 60° fibre oriented composites. In particular, carbon fibre composites with 0° fibre orientation displayed a maximum tensile strength of 165 MPa.

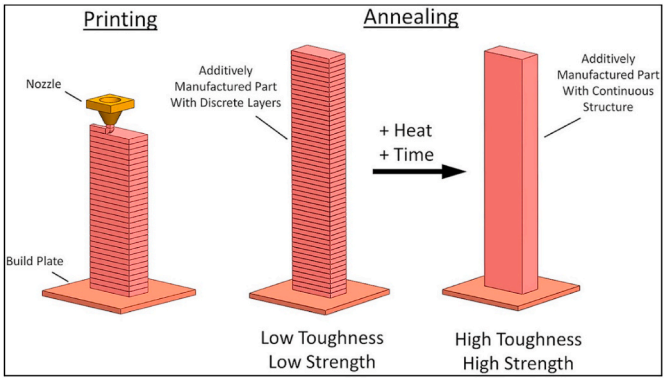

Fig. 6. Annealing process after printing, reproduced with permission from Ref. [77].

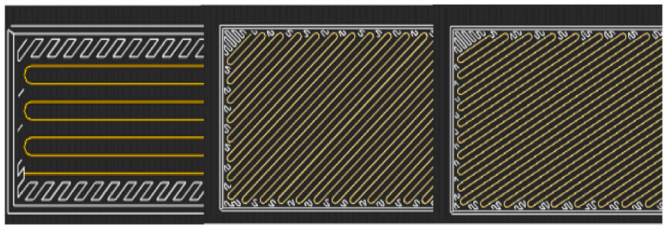

Fig. 7. Fibre orientation 0°, 45°, and 60° for different test specimens, reproduced with permission from Ref. [102].

4. Fibre matrix interface and its significance in FDM part performance

The characteristics and properties of the fibre composites in AM not only depend on the printing parameters and materials used but also on the interfacial bonding developed between fibre and matrix. The interaction between the fibre and the matrix is crucial for the efficient transfer of load and stress. The interfacial bonding characteristics can be varied by changing the fibre orientation, by varying fibre content, and by introducing fibre treatments. Parandoush et al. [103] developed a laser-assisted AM method, whereby an excellent interfacial bonding was developed between the glass fibre and PP. The tensile properties of the samples printed by the proposed method were higher than those of the traditional FDM printed short fibre composites with 300% and 150% increase in tensile strength and modulus, respectively. Liu et al. [104] studied the sizing effect on a carbon fibre composite. The sizing method was done using a water-based polyamide solid dispersion emulsion sizing agent PA845H. Sized carbon fibre improved the interfacial bonding between the fibre and matrix, which improved the flexural strength by 82%, flexural modulus by 246%, and interlaminate strength by 42.2%. Fig. 8 shows the mechanism behind the enhanced fibre matrix interface due to the sizing treatment. In another study, the addition of glass fibre to PP filament increased the adhesion of the layers, which reduced the shrinkage and bend as compared to pure PP material [105]. Bonding between successive layers and voids are the major concerns in FDM prototypes and these factors are directly integrated with the mechanical strength of the parts.

Yao et al. [106] investigated the tensile and flexural properties of continuous carbon fibre reinforced PLA composites. Composites were printed with 20% infill density and varying carbon fibre filaments (3 K, 6 K, and 12 K filaments). Carbon fibre composites showed a higher tensile and flexural strength than that of the pure PLA. However, the author found that the lack of adhesion between the fibre and the matrix resulted in carbon fibre debonding from the matrix leading to reduced tensile and flexural strength. This was due to the lack of chemical bonding between PLA and carbon fibre. In order to improve the chemical bonding between the matrix and the fibre, the author recommended surface modification of carbon fibre. Interfacial adhesion is a critical factor in affecting the modulus of carbon fibre PP composite [107]. Weak bonding in the carbon and wood fibre reinforced PLA composites reduced the load-carrying ability of the PLA that correspondingly reduced the tensile modulus and strength [108]. To achieve enhanced performance in the FDM printed biocomposite, it is necessary to tailor the interfacial bond strength as well as the choice of fibre and matrix material [109].

Through variation in the fibre direction, it is possible to increase the fibre-matrix interaction [110]. Ning et al. [111] reported that bonding between the layers was reduced when increasing the printing layer thickness above 0.25 mm.

Li et al. [112] designed a nozzle for uniform reinforcement of carbon fibre in PLA matrix during FDM printing. Pre-processed carbon fibre with a PLA sizing agent effectively increased the interfacial strength between carbon fibre and PLA. It is observed that the modified carbon fibre reinforced composites showed higher tensile and flexural strength, which was 14% and 164% higher, respectively than the unmodified carbon fibre reinforced composite. The short carbon fibre reinforcement restricted the flow of ABS matrix during FDM, consequently developing voids and pores in the composite, which reduced the interfacial adhesion between fibre and matrix [113]. Tian et al. [114] developed continuous carbon fibre/PLA composites printed through FDM process and found that the layer thickness of 0.4–0.6 mm and the hatch spacing of 0.6 mm are capable of producing guaranteed bonding between the printed layers. Specifically, the layer thickness of 0.5 mm exhibited homogeneous bonding between the deposited layers, which increased the fibre matrix interface accordingly. Fibre treatment with a silane coupling agent is an efficient way to develop enhanced bonding between basalt fibre and PLA matrix [115]. Zhu et al. [116] used random terpolymer-copolymer of styrene, acrylonitrile, and glycidyl methacrylate as a compatibiliser to make ABS short carbon fibre composites. Compatibiliser was added with varying weight percentages of 0, 1, 3, 5, and 7 wt %. The addition of the compatibiliser had shown a significant improvement in the interfacial characteristics. Due to the increased bonding of the compatibiliser added composites, the tensile and flexural strength was observed to be higher than that of the composite without the compatibiliser. The strong interface between carbon fibre and the compatibiliser was the result of chemical bonding between glycidyl methacrylate in the compatibiliser and hydroxyl-carboxyl groups in the carbon fibre. The compatibiliser had a molecular structure similar to that of the styrene-acrylonitrile copolymer in ABS, thus achieving good physical compatibility between ABS and the compatibiliser. Heidari-Rarani et al. [117] observed delamination on carbon PLA composite fractured surface owing to the poor permeability of the molten PLA into the carbon fibre bundle. In order to increase the permeability of PLA to the carbon bundle, the author recommended surface treatment of the fibre. Chacón et al. [118] found extensive carbon fibre pull-out on tensile fractured carbon/PA composites due to poor interfacial bonding between PA-matrix and fibre. Internal fibres were barely infiltrated by the PA-matrix and only a limited number of external fibres were found to be in contact with the PA-matrix, which was the main reason for poor bonding. It can be understood from the available literature that the variation in the fibre structure and length, fibre treatment, and addition of compatibiliser and coupling agents could improve the fibre-matrix bonding. Moreover, no modelling work was found to be performed on the fibre-matrix bonding in FDM of AM. In this view, it is necessary to develop models to understand the fibre-matrix bonding in FDM parts/composites, through which the physical properties of the composites can be easily predicted.

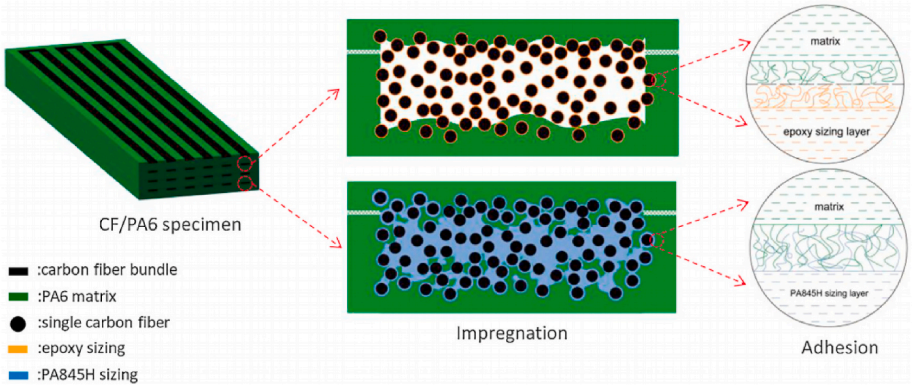

Fig. 8. Interface enhancement mechanism due to sizing treatment, reproduced with permission from Ref. [104].

5. Mechanical testing and performance

5.1. Standards for FDM polymer/composite testing

ASTM and ISO testing methods are used to test the properties of AM polymers. Two organisations have been involved in setting standards and testing procedures for AM polymers. F42 Committee and its sub-committee F42.05 in ASTM have the authority over AM materials and TC261 for ISO standards [119]. These two groups are currently engaged in setting mechanical testing standards for AM products and parts through comparison with existing specifications. In 2014, ISO has published standard methods and test techniques for AM parts, indicating the fundamental quality attributes of the parts, specifying the suitable test methodology, and specifying the scope and content of the test and supply agreements [120]. Standards followed for conducting tensile, flexural, impact, and compression tests on FDM based polymers and composites are shown in Table 2. The tensile test can be performed on both the dumbbell-shaped and the flat/straight bar-shaped specimens. For the impact test, both notched and un-notched specimens can be used, however, there is no clear indication whether the notch should be made during or after printing.

5.2. Tensile properties of fibre composites fabricated through the FDM process

In many industries, AM process utilisation is expanding rapidly owing to its flexibility in manufacturing complex designs. The recent development of fibre composites through FDM process broadens the research options in this field. Factors such as fibre reinforcement, fibre content, and printing parameters significantly affect the tensile properties of the composite. The tensile strength of the FDM printed composite is the function of fibre reinforcement percentage and fibre orientation [121]. The FDM printed fibre composite exhibit anisotropic mechanical properties due to the variation in bonding between layers. The anisotropic mechanical properties of the printed fibre composites affect the final component output [122]. To increase the application of these composites, it is necessary to understand the composites' tensile behaviour, which enables identification of optimum features in the manufacturing of fibre composites and consequently develop a guideline to design 3D printed fibre composites. There are several studies that conducted tensile test on the FDM manufactured fibre composites. Zhong et al. [19] suggested reinforcement of short fibre to the ABS matrix to increase the tensile strength of FDM printed composites. Ning et al. [123] studied ABS composite reinforced with carbon fibre at varying weight percentages (3%, 5%, 7.5%, 10%, and 15%). The carbon fibre was reinforced in two different sizes of 150 and 100 μm. The addition of carbon fibre improved the tensile strength by 20–30%. The maximum tensile strength (42 MPa at 5 wt% carbon fibre content) and Young's modulus (2.5 GPa at 7.5 wt% carbon fibre content) were noted for the composite with 150 μm carbon fibre reinforcement. This investigation provides a clear view of the short fibre reinforcement effect on the tensile properties of ABS composite, although the fracture mechanism has not been compared between the two different fibre lengths. Liao et al. [124] investigated the tensile properties of short carbon fibre (15–20 mm in length) reinforced PA12 composite fabricated with the different mass fractions of carbon fibre (2, 4, 6, 8, and 10 wt%). Carbon fibre reinforcement at 10 wt% showed superior tensile strength, which is over 100% higher than the pure PA12. Li et al. [125] fabricated PLA composite with short carbon fibre (100–150 μm) by varying layers. The composite with one layer of pure PLA and other layers of carbon fibre PLA showed a maximum tensile strength of 56 MPa, which was 1.16 times higher than the pure PLA polymer. Overall, these investigations show the efficacy of short fibre reinforcement in FDM printed composites. However, in all these investigations, the length of the fibre was not varied in an effective way to analyse the influence of the fibre length on tensile properties. Thus, more investigations are necessary that could lead to the finding of an optimum short fibre length in order to achieve maximum tensile strength and modulus.

Tekinalp et al. [70] investigated ABS composite fabricated through FDM and compression moulding method. The short carbon fibre of length 0.2–0.4 nm was used for reinforcement. The tensile strength of the ABS composite was found to be low for the composite fabricated through FDM. In FDM composites, the formation of voids and pores is higher than the traditional manufacturing methods, and the reduction of such voids and pores can produce comparable results between FDM printed and traditional manufactured composites. In such a view, Keles et al. [126] manufactured the short carbon fibre reinforced ABS composite through a vibration-assisted FDM method. Inducing vibration in the extrusion head during fabrication reduced the formation of voids and pores, which correspondingly increased the modulus and strength. Shofner et al. [127] reported that the addition of short carbon fibre (100 μm) to ABS polymers changed the properties of the ABS material from ductile to brittle due to non-homogeneous bonding between layers as well as between fibre and matrix. The tensile fracture characteristics exemplify the increased stiffness of the composites developed by the reinforcement of the fibre. Fibre reinforcement inhibits the mobility of the polymer chain, thus increasing the stiffness of the composite. Moreover, the authors recommended the treatment of fibre to enhance the mechanical properties of 3D printed composites. Zhang et al. [113] reported that matrix fracture, fibre debonding, fibre pull out and weak fibre-matrix interface were found to be the dominant tensile failure modes of short carbon fibre composite. Mori et al. [128] successfully fabricated sandwiched ABS composite having 1.4 vol% of long carbon fibre (70 mm) reinforcement. The composite exhibited the maximum tensile strength of 43 MPa, which was 3–4 times higher than the pure ABS material. However, the fracture mechanism involved in the failure of long fibre composites was not disclosed in this study. Long fibre reinforced composites are expected to provide increased tensile strength than short fibre composites due to a higher area of interfacial interaction. In order to prove this, it is necessary to carry out a comparative study that would provide insight into the aforementioned fact. Magri et al. [129] investigated the effect of FDM printing parameters on the tensile properties of short fibre PLA composites. Composite printed at nozzle temperature of 230 °C and infill line orientation of 0°/15°/-15° showed a maximum tensile strength of 36 MPa. This study demonstrated the influence of the nozzle temperature and the infill line orientation on the tensile strength, however, these parameters have not yet been optimised for maximum tensile strength and modulus. Other parameters, such as infill density, raster angle, and layer thickness, are also expected to have a significant effect on tensile properties. To prove this, Ning et al. [111] investigated the tensile characteristics of carbon fibre composites with respect to varying printing parameters, raster angle, infill speed, nozzle temperature, and layer thickness. Composite printed at a raster angle of 0°/90° showed maximum tensile strength whereas

Table 2
The testing standard followed for testing FDM based polymers [119,120].

S.No	Test	Standard
1	Tensile	ASTM D638 (P) ISO 527-2 (P) ASTM D3039 (C) ISO 527-4 (C)
2	Flexural	ASTM D790 (P/C) ISO 178 (P/C) ASTM D7264 (C)
3	Impact	Charpy Impact (Notched) ASTM D6110, ISO 179 (P/C) Izod Impact (Notched) ASTM D256, ISO 180 (P/C) Izod Impact (Unnotched) ASTM D4812, ISO 180 (P/C)
4	Compression	ASTM D695 (P) ISO 604 (P) ASTM D3410 (C) ISO 14126 (C)

P – polymer, C- composite.

maximum modulus was noted at a raster angle of −45°/45°. Infill speed of 25 mm/s led to increased tensile strength, modulus and yield strength. Lower nozzle temperature was recommended to achieve strong bonding of the layer and increased tensile strength.

Continuous fibre is the most effective reinforcement for fabricating high strength fibre reinforced thermoplastic composite through FDM [130,131]. The maximum tensile strength and modulus of FDM printed continuous fibre composites reported in different literature are as follows. Compared to pure PLA, PLA composite with 6.6% of continuous carbon fibre reinforcement shows 599% and 435% increment in the tensile modulus and strength, respectively [132]. Hao et al. [133] fabricated continuous carbon fibre reinforced epoxy composite through FDM. The tensile strength of the carbon epoxy composite was 792.8 MPa, which was higher than the thermoplastic PLA carbon fibre composite. Addition of 9.5 wt% of continuous aramid fibre in PLA polymer increased the tensile strength and modulus by 499 and 186%, respectively [110]. Yao et al. [106] fabricated PLA composite with 3 K, 6 K, and 12 K continuous carbon fibre reinforcement. The tensile strength was found to be improved by 38.68%, 58.86%, and 70.02% for 3 K, 6 K, and 12 K carbon fibre composite, respectively. Der Klift et al. [134] studied the effect of continuous carbon fibre reinforcement in the PA matrix. The composite was fabricated with varying fibre volume percentages. The composite with 6.9% of fibre exhibited maximum tensile strength (464 MPa) and modulus (35.7 GPa). ABS composite with 10 wt % continuous carbon fibre exhibited improved tensile strength of 147 MPa when compared to the pure ABS polymer [135]. From these results, continuous fibre reinforcement of 5 wt% to 10 wt% in FDM polymers showed improved tensile strength and modulus. However, when the loading amount of fibre increases, the brittleness of the composite filament increases too, making printing difficult. In order to increase the flexibility of the filaments, Sodeifian et al. [105] added maleic anhydride polyolefin (POE-*g*-MA) at varying weight percentages (10, 20, and 30 wt%) to PP composite filaments having 30 wt% of glass fibre reinforcement and composites were subsequently printed. The tensile test results of the printed PP/glass fibre/POE-g-MA composites are shown in Fig. 9. The addition of glass fibre to the PP filament increased the modulus of the composite as well as the elongation at break. The addition of POE-g-MA to glass fibre composite reduced the tensile strength. The addition of 10 wt% and 2 wt% of POE-g-MA increased the flexibility of the composites, but POE-g-MA at 30 wt% showed reduced flexibility, compared to the PP/GF specimen without POE-g-MA. Table 3 presents the tensile strength of some FDM fabricated fibre composites.

To understand the stress concentration effect on the FDM printed continuous fibre composites, Pyl et al. [140] conducted an open-hole tensile test on the carbon PA composite printed in rectangular as well as dumbbell shape. Four specimens were studied, namely, dumbbell and rectangular specimens with printed hole and dumbbell and rectangular specimens with drilled hole. High-stress concentrations were observed in all the specimens near the 'hole' area during tensile loading. Under increasing load, cracks and fibre damage from the stress-concentrated points propagated leading to failure. FDM printed parts have sharp edges and corners, which may increase stress concentration. Thus, necessary modelling tools need to be developed to predict stress concentration that could reduce the chances of failure due to stress concentration. Fig. 10 compares the tensile strength of FDM printed composites tested at different strain rates.

Dong et al. [141] studied the kevlar fibre reinforcement effect in the PA matrix. The fibre was reinforced at different layering patterns and

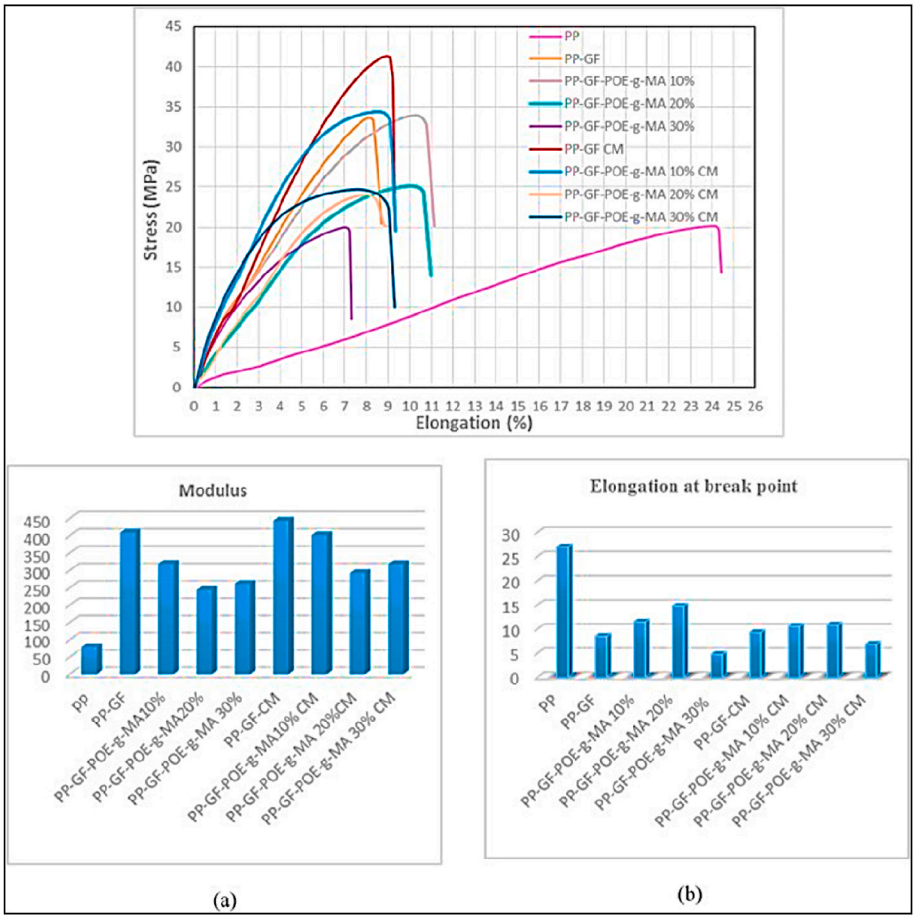

Fig. 9. Tensile test results of PP/glass fibre/POE-g-MA composites, reproduced under the. terms of the Creative Commons Attribution (CC-BY) license from Refs. [105].

Table 3
Tensile and flexural propertiesof FDM fabricated fibre composites.

Matrix	Reinforcement	Material	Tensile Properties				Flexural Properties				Reference
			Max. tensile strength (MPa) @ wt.%	% of Enhancement compared to pure resin	Max. tensile modulus (GPa) @wt.%	Elongation at break compared to pure resin	Max. flexural strength (MPa) @ wt.%	flexural strength compared to pure resin	Max. flexural modulus (GPa) @wt.%	flexural modulus compared to pure resin	
PLA	Modified-CCF	The **novel Extrusion nozzle and path control methods** were designed to print curved CCF/PLA composite.	91	13.8% higher than original CCF/PLA composites	–	–	156	164% higher than original CCF/PLA composites	–	–	[112]
PLA	Basalt fibre	**KH550-treated** basalt fibre (KBF) reinforced PLA composite	72 @ 20 wt% of KBF	33%	5.55 @ 20 wt% of KBF	Continuously decreased	131 @ 20 wt%	Increased	5.08 @ 20 wt%	Increased	[115]
	Carbon fibre (CF)	CF reinforced PLA composite	69 @ 10 wt% of CF	27%	7.18 @ 20 wt% of CF		117 @ 5 wt%	Decreased	–	Increased	
ABS	Short carbon fibre	SAG **compatibiliser** added short carbon fibre (SCF)/ABS composites	73.3 @ 5 wt% of SAG	15.4% higher than 0 wt% of SAG	–	Increased up to 5 wt% SAG addition (23.8%) and then decreased	18.7% improved flexural strength @ 3 wt% of SAG addition than 0 wt% of SAG		3.2% improved flexural modulus @ 3 wt% of SAG addition than 0 wt% of SAG		[116]
PLA	CCF	An **innovative extruder** is designed and manufactured for FDM 3D printers to produce CCF reinforced PLA composites.	61.4	37%	8.28	Reduced	152.1	109% increased	13.42	368% increased	[117]
ABS	CF	Different **content** and **length** of CF added ABS composites	42 @ 5 wt % of CF	23%	2.5 @ 7.5 wt% of CF	–	11.82% improved flexural strength @ 5 wt% of CF reinforcement than pure ABS		16.82% improved flexural modulus @ 5 wt % of CF reinforcement than pure ABS		[136]
PA12	CF	**Different content** of CF added ABS composites	93.8 @ 10 wt% of CF	102.2%	3.58 @ 10 wt% of CF	Continuously decreased	124.9 @ 10 wt% of CF	251.1% increased	5.25 @ 10 wt% of CF	346% increased	[124]
ABS	CCF	10 wt% of CCF/ABS composites and compared with **Injection moulded** samples	147 @ 10 wt% of CCF	5 times higher	4.18 @ 10 wt% of CCF	2 times higher	127 @ 10 wt% of CCF	2 times higher	7.72 @ 10 wt% of CCF	3.9 times higher	[135]
PLA	Glass fibre (GF)	In-melt continuous glass fibre yarn embedded PLA composites and **theoretical validation**	478 @ 50 vol% of GF	–	29.4 @ 50 vol% of GF	–	–	–	–	–	[131]
PLA	CF	CF/PLA composites with different content and two bead lay-up	54.64 @ 5 wt% of CF	12.4%	–	–	–	–	–	–	[101]
PLA	CCF	**Recycling and remanufacturing** of 3D printed CCF/PLA composites	256 @ 10 wt% of CF	4 times higher	20.6 @ 10 wt% of CF	–	263 @ 10 wt% of CF	≈2.6 times higher	13.3 @ 10 wt% of CF	≈3 times higher	[137]
r-PP	hemp fibres	Composite filaments comprising of pre-consumer recycled PP with varying contents of hemp fibres were extruded	34 @ 30 wt% of hemp	54%	2.16 @ 30 wt% of hemp	Reduced	–	–	–	–	[138]
PEEK and ABS	–	The influence of layer thickness and raster angle on the mechanical properties of 3D-printed PEEK and compared with ABS	56.6 @ 300 μm of layer thickness	108% higher than ABS	–	–	56.2 @ 300 μm of layer thickness	15% higher than ABS	1.6	–	[139]

Note: SAG: styrene, acrylonitrile, and glycidyl methacrylate; CCF: Continuous Carbon Fibre; **Bold:** the novelty of the work.

infill angles. The investigation reported a maximum elastic modulus of 27 GPa and strength of 333 Mpa for the composite fabricated at 0° infill angle and 18 layers of fibre. The variation in the infill angle did not show any significant effect on the modulus.

Various researchers have also studied the tensile properties of natural fibre reinforced FDM composites. Milosevic et al. [138] investigated 30 wt% hemp fibre reinforcement effect in the PP matrix. The composite exhibited 50% and 143% improvement in the tensile strength and modulus, respectively when compared to the pure PP. In another work, Stoof et al. [142] investigated harakeke fibre reinforced PLA composite's tensile strength. Composites were printed at different fibre weight percentages. The composite with 20 wt% harakeke fibre reinforcement showed maximum tensile strength, which was 5.4% higher than the pure PLA polymer. Matsuzak et al. [132] made a comparison on the tensile characteristics of PLA composite reinforced with jute fibre and carbon fibre. Compared to PLA, carbon fibre composite exhibited 425% and 599% increase in the tensile strength and modulus, respectively whereas the jute fibre composite showed 157% and 134% increment for

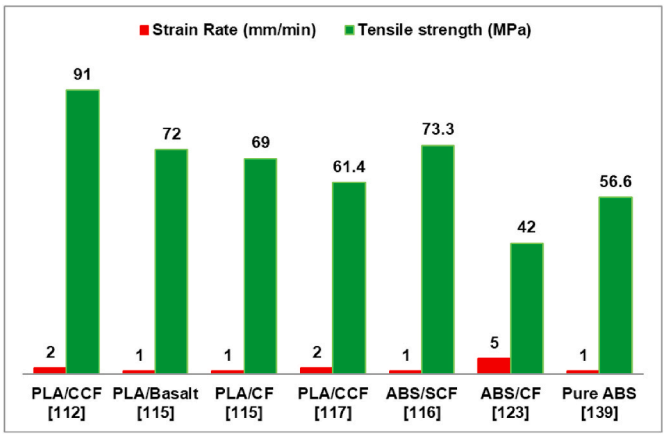

Fig. 10. Tensile strength of FDM printed composites tested at different strain rates. (CF - carbon fibre, CCF - continuous carbon fibre, SCF - short carbon fibre).

the same properties. Duigou et al. [143] investigated flax fibre-reinforced PLA composite with 30% fibre volume content and suggested continuous reinforcement of natural fibre for enhancing mechanical performance. The tensile properties exhibited by FDM printed natural fibre composites are satisfactory and enhanced research in this area could increase the application of natural fibres in 3D printing technology. A few researches have also been conducted on the area of hybridised composites manufactured by FDM. Oztan et al. [144] investigated kevlar and carbon fibre reinforced PA composite's tensile property. The composites exhibited linear-elastic behaviour under the tensile loading. During loading, the failure of the composite occurred within 1.4–2.5% of strain. Sang et al. [115] compared the tensile strength of the carbon fibre/PLA composite and silane treated basalt fibre/PLA composite. Both carbon fibre and basalt fibre were loaded in three varying weight percentages of 5, 10, and 20%. Silane-treated basalt fibre composite showed a tensile strength comparable to that of carbon fibre composite. 20% basalt fibre composite had a maximum tensile strength of 72 MPa, which is approximately 33% higher than the pure PLA (54.2 MPa). These results demonstrate the possibility of developing high-strength hybrid composites through FDM.

5.3. Flexural properties of fibre composites fabricated through the FDM process

In FDM manufactured fibre composites, the interlaminar shear strength is compromised, which directly affects the flexural strength of the composites. The anisotropic properties of the FDM fabricated fibre composite under bending cause variation in the strain rate, which increases the shear stress between the layers leading to the separation of the layers and eventual failure. Interlaminar shear strength is a critical component to be focused on improving the flexural character of FDM fibre composite. Flexural properties of FDM printed fibre composites are shown in Table 3. Li et al. [125] explored the impact of short-carbon fibre reinforcement on the PLA composite. The length of the fibre was maintained between 100 and 150 μm and the volume of reinforcement was 15 vol%. The maximum flexural strength and modulus of the PLA carbon fibre composite was 74 MPa and 21 GPa, respectively. A uniform distribution of flexural load from PLA to carbon fibre was observed, which is the key explanation for increased flexural strength. However, the influence of varying fibre percentages was not disclosed by the authors, which could aid in finding the optimum level of fibre percentage for maximum bending strength. In this regard, Gavali et al. [145] found an increment in the flexural strength of the chopped carbon fibre PLA composite owing to the increment in carbon fibre reinforcement. The PLA exhibited flexural strength of 66 MPa and on reinforcing 10 wt% of carbon fibre, the strength increased to 67 MPa. When the weight percentage increased to 15%, the flexural strength was ca. about 78 MPa.

Goh et al. [146] investigated PA composite reinforced with continuous glass and carbon fibre. Compared to the glass fibre composite, carbon fibre composite exhibited maximum flexural strength (430 MPa) and flexural modulus (38.1 GPa). The maximum flexural strength and flexural modulus reported for glass fibre composite were 149 MPa and 14.7 GPa, respectively, approximately 40% of the strength and modulus of carbon fibre composite. Yao et al. [106] analysed the flexural strength of the carbon fibre PLA composites having carbon fibre with varying tow (3 K, 6 K, and 12 K). The increase in the carbon fibre tow increases the flexural strength and modulus of the PLA and carbon fibre composites. Maximum flexural strength of 68 MPa was noted for the 12 K carbon fibre/PLA composite, for 3 K and 6 K it was 60 and 66 MPa respectively.

Tian et al. [114] studied the flexural characteristics of the continuous carbon fibre reinforced PLA composite. Composites were printed with varying FDM-printing parameters of layer thickness, liquefier temperature, filament feed rate, hatch spacing, and printing speed. Interestingly, flexural strength and modulus increased steadily when the liquefier temperature increased from 180 to 240 °C. When the liquefier temperature was 240 °C, the maximum flexural strength (335 MPa) and the modulus (30 GPa) were recorded. However, the increasing trend in layer thickness and hatch spacing reduced the flexural modulus and strength. There is no significant variation in flexural strength and modulus at varying printing speeds. This investigation demonstrated the influence of printing parameters on the flexural properties of FDM composites, however, the orientation of the fibre was not considered in the investigation. Variation in fibre orientation affects the bending nature of FDM composites. In this view, Araya-Calvo et al. [158] investigated continuous carbon fibre PA composite and found significant variation in the flexural properties of the composites on varying print orientation and reinforcement type. In another work, Chacón et al. [118] investigated the influence of build orientation on the flexural strength of FDM composites. Fig. 11 shows the flexural stress-strain curves of the PA composites having glass, kevlar, and carbon fibre reinforcement fabricated with different build orientations. These results showed that flat build orientation maximised the flexural property of all the composites. Compared to Kevlar and glass fibre reinforcement, carbon fibre composite showed maximum flexural strength. The maximum flexural strength of 424 MPa and the flexural modulus of 39 GPa was reported for carbon fibre composites with a flat orientation. Fig. 12 compares the flexural strength of FDM printed composites tested at different strain rates. Hu et al. [147] examined the variation in flexural property of the PLA carbon fibre composite at varying layer thickness, printing speed, and printing temperature. The results reveal the influence of layer thickness on the flexural modulus and strength. The maximum strength of 610 MPa and modulus of 40 GPa was obtained at a combination of high printing temperature, low layer thickness, and low printing speed. Overall, these studies highlight the importance of optimising the FDM variables for the bending properties of fibre composites. However, FDM involves a number of variables, along with fibre and polymer properties, making optimisation challenging. In the case of short fibre composites, Spoerk et al. [94] observed variations in flexural properties of 250 μm-short carbon fibre composite with respect to variation in the fibre orientation. Variation in fibre orientation significantly improved the flexural strength and modulus of PP and short carbon fibre composites by 150% and 400%, respectively. Maximum flexural strength of 51 MPa was noted on the composite printed at 0°/90° orientation and the corresponding flexural modulus was 3385 MPa. In addition, the authors recommended the addition of compatibilisers for PP-based composites in order to achieve uniform dispersion of the fibre as well as enhanced fibre matrix bonding that would increase the bending strength. Surface modification of fibre could also increase the fibre matrix interfacial bonding. Sang et al. [115] reported that the silane treated basalt PLA composite exhibited enhanced flexural properties compared to the carbon fibre composite. The carbon fibre reinforcement increased the

matrix viscosity, which reduced the printing flow-ability and bonding between the adjacent layers, consequently reducing the flexural strength of the composite. The silane-treated 20 wt% basalt fibre composite exhibited the highest flexural strength of 131 MPa and flexural modulus of 5.08 GPa.

5.4. Impact properties of fibre composites fabricated through the FDM process

Fibre composite impact strength is critical to address the stiffness and strength of composites against impact loads in applications such as automobiles. A sudden impact on the fibre composite could produce fibre-matrix debonding, fibre delamination, and fibre breakage, which could lead to failure in load transmission. In 3D printed fibre composites, the impact strength depends on the interfacial bonding as well as the fibre content. Most of the literature in the 3D fibre composites investigated the composite's tensile and flexural properties but the impact behaviour of the 3D printed fibre composites remains to be investigated systematically. Only limited studies have reported the impact characteristics of the fibre composites fabricated through the FDM process. Knowledge of the impact strength of 3D printed composites would expand their application in the automobile sector.

Chacón et al. [118] investigated the tensile and flexural properties of the 3D printed PA composites with continuous carbon, glass, and Kevlar reinforcement and stated that investigating the impact performance of the 3D printed fibre composite would bring possibilities for their usage in various applications. Caminero et al. [148] investigated the impact strength behaviour of PA composites with continuous glass, kevlar, and carbon fibre. Composites were printed at flat and on-edge orientations. The carbon fibre composite exhibited poor impact strength owing to the increased brittleness of carbon fibre whereas the glass fibre composite exhibited maximum impact strength. However, when increasing the carbon fibre content, the composite impact strength was increased considerably. The maximum impact strength was noted for on-edge printed composites with 34 vol% of fibre, i.e. compared to flat orientation printed composites, on-edge printed PA composites with carbon fibre showed a 43% increase in impact strength, 47% for Kevlar fibre and only 4% for glass fibre reinforcement. Tian et al. [137] investigated the impact strength of the PLA composite with 10 wt% of continuous carbon fibre. The pure PLA and carbon fibre reinforced PLA exhibited impact strengths of 20 kJ/m^2 and 35 kJ/m^2, respectively. The author claimed the variation in the impact strength was not a multifold improvement. The limited increase in the strength was attributed due to the lower strain of the carbon fibre. On impact, the carbon fibre was found to be fractured and pulled out of the matrix. Liao et al. [124] analysed PA12/long carbon fibre (15–20 mm) composite impact strength behaviour at the varying fibre contents (2, 4, 6, 8, and 10 wt%). From 2 to 8 wt% carbon fibre reinforcement, the impact strength was

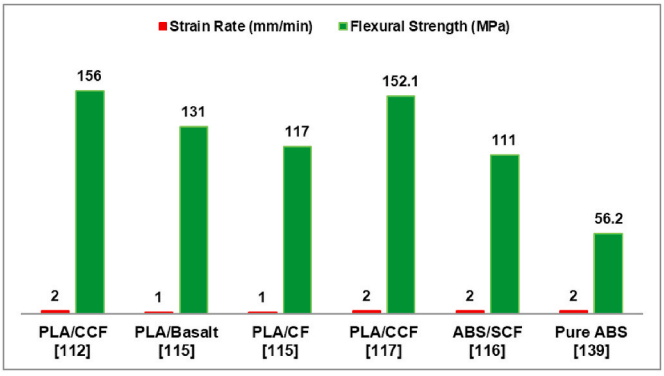

Fig. 12. Flexural strength of FDM printed composites tested at different strain rates. (CF - carbon fibre, CCF - continuous carbon fibre, SCF - short carbon fibre)

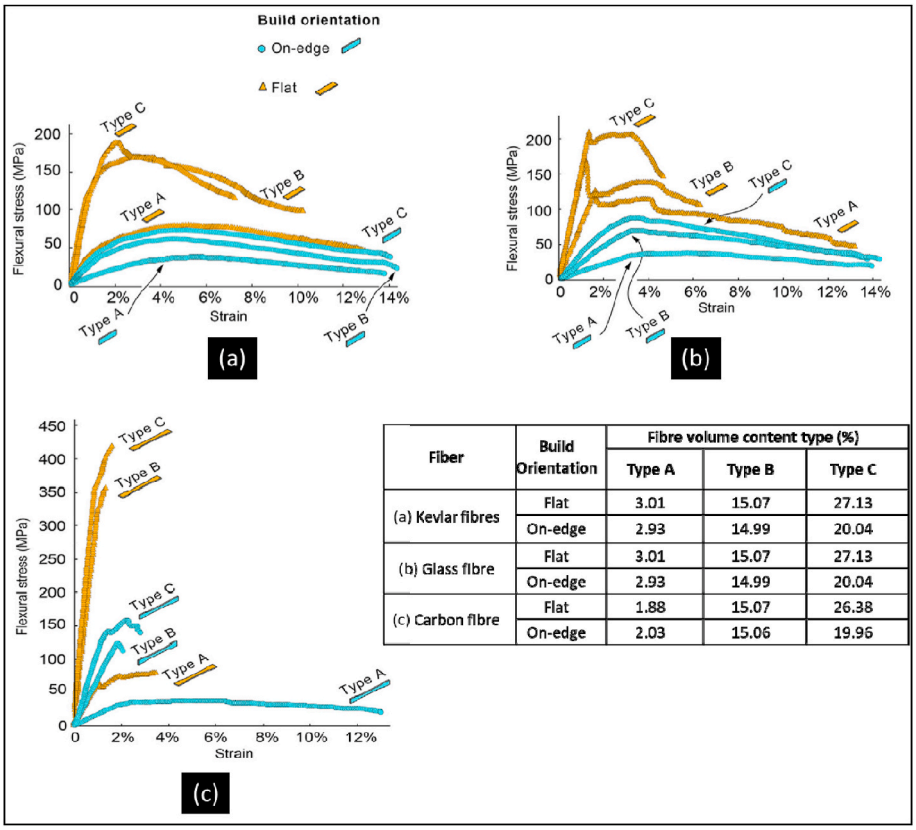

Fiber	Build Orientation	Fibre volume content type (%)		
		Type A	Type B	Type C
(a) Kevlar fibres	Flat	3.01	15.07	27.13
	On-edge	2.93	14.99	20.04
(b) Glass fibre	Flat	3.01	15.07	27.13
	On-edge	2.93	14.99	20.04
(c) Carbon fibre	Flat	1.88	15.07	26.38
	On-edge	2.03	15.06	19.96

Fig. 11. Flexural test stress-strain curves of fibre-reinforced PA-composite (a) kevlar fibre (b) glass and (c) carbon fibre, reproduced with permission from Ref. [118].

lower than the pure PA material owing to the penetration of stress concentration at the end of the fibre, which leads to crack initiation during impact. At 8 and 10% carbon fibre reinforcement, the composite developed crack resistance ability. The maximum impact strength was noted for the 10 wt% carbon fibre composite, which was 10% higher than the pure PA12 material. Except for the 10 wt% carbon fibre reinforced composites, the other composites displayed lower impact strength than the pure PA12. These results indicate that the type and amount of reinforcement is important for enhancing impact strength and carbon fibre composites have a low impact strength due to the brittle nature of the carbon fibre. Similarly, in another study, short carbon fibre reinforcement increased the brittleness of the PP matrix, which led to brittle fracture under impact load. 10% carbon fibre reinforced composite exhibited two to four times lower impact strength than the PP material [94]. However, Ashori et al. [107] have achieved improved impact strength in short carbon fibre/PP composites by coating carbon fibre with exfoliated graphene nanoplatelets (xGnP). Carbon fibre was reinforced at 15 wt% and coating was made at three different percentages (0.5, 1, and 3 wt%). The maximum impact strength was noted for the 1 wt% xGnP coated composite, which was 7% higher than the uncoated composite. During impact, the xGnP coating minimised the chances of crack initiation and propagation. The impact strength of cork granules reinforced PLA composite was investigated by Daver et al. [149]. Composite was fabricated with varying percentages of cork granules reinforcement. The addition of cork granules in PLA material reduced the impact strength of the composite. The impact strength was found to be low at all weight percentages, but the addition of the plasticiser in the form of tributyl citrate to the cork PLA composite significantly increased the impact strength compared to the pure PLA material. Overall, it is understood that the impact strength of FDM printed fibre composites is low, and this shortcoming can limit the application of FDM printed parts in automobile sectors. In order to address this, research in this field should be expanded in a different approach to optimise the FDM parameters and base material as well as the reinforcement properties. The impact strengths of various FDM printed fibre composites is shown in Table 4.

5.5. Compression properties of FDM fibre composites fabricated through the FDM process

FDM manufactured fibre composites exhibit poor compressive strength due to their anisotropic and brittle nature making it is necessary to study resistance to compressive load behaviour. The layer of the FDM printed material debonds and undergoes plastic deformation under compression load. The compressive loading of the FDM parts may cause layer separation and increased buckling [18]. Justo et al. [56] observed the failure mechanism for PA composites with glass and carbon fibre reinforcement. Carbon fibre failed before the buckling of the composite, however, the failure of the glass fibre was noted after the buckling of the composite. Material buckling is categorised as the main failure mode of 3D printed fibre composites under the compression load [154]. Hou et al. [155] investigated continuous kevlar fibre reinforced PLA composite at varying fibre percentages and reported that 11.5% of fibre reinforcement produced an increased compressive strength of 17 MPa in the PLA matrix. The authors observed that during compression loading, the composite experienced elastic buckling and plastic deformation. Using FDM 3D printing techniques, two different sandwich composites were manufactured with vertical pillar corrugated sine wave (VPSC) structure and vertical pillar corrugated trapezoidal (VPTC) structure, made of PA/glass fibre and photopolymers (80% rigid-ABS, 20% Flexible-Rubber) [154]. Composite with the VPSC structure showed good compressive strength compared to the VPTC structure. It is understood that, due to their anisotropic nature, fibre composite materials are more likely to buckle under compression loading and eventually lead to greater deformation or even crippling of the material. However, reinforcement of continuous fibre in FDM polymers is observed to significantly reduce buckling during compression loading conditions. The SEM morphology of the sample tested for compression showed buckling and separation of layers as major failure modes during loading (Fig. 13). De-bonding of layers under compressive load is another failure mode. De-bonding affects the general stress-strain behaviour of the composite resulting in poor compressive strength. Proper amendment of process parameters (optimised process parameters) during the manufacturing of fibre reinforced composites significantly influences the layer bonding, which correspondingly improves the compressive strength of the composites.

Kaur et al. [156] investigated the compressive strength of 3D truss structure made of polymeric materials PA618, PLA, and carbon fibre reinforced PLA by the FDM 3D printing process. In the uniaxial compression test, the stress-stress curve showed significant stretch dominance behaviour for polymeric materials at different strain rates. Carbon fibre PLA composite showed promising mechanical stability compared to pure PA618 and PLA. In another work, compressive properties of aramid fibre reinforced PLA were compared to pure PLA by Bettini et al. [110]. The results showed an 87% increase in compressive strength when reinforcing PLA with aramid fibre. Improper feeding of fibre in accordance with the speed of extrusion during the FDM process breaks the fibre and results in homogeneous extrusion and clogging. In the case of continuous fibre reinforcement FDM, variable extrusion speed plays a vital role in the printed composite compression performance under loading conditions.

In order to achieve maximum compressive strength in ABS-P400 [157], FDM process parameters of layer thickness, raster angle, raster width, orientation, and air gap were analysed. The Quantum-behaved particle swarm optimisation (QPSO) technique was used to optimise the process parameters. The maximum compressive stress of 17.48 MPa was achieved under printing conditions of 0.254 mm layer thickness, 0.036° orientation, 59.44° raster angle, 0.422 mm raster width, and 0.00026 mm air gap. Araya-Calvo et al. [158] investigated the compression strength of the PA6 composite made of continuous carbon fibre reinforcement. The compression strength was analysed at different fibre percentages, which varied according to the type of reinforcement (isotropic and concentric), reinforcement orientation, and print orientation (parallel and perpendicular to the direction of force). A significant influence of the reinforcement distribution and the reinforcement type on the compression response was noted from the investigation. The maximum compressive response was observed at 0.25 carbon fibre volume ratio, resulting in a compressive modulus of 2.102 GPa and compressive stress at a proportional limit of 53.3 MPa. The distribution of reinforcement material has a significant role to play in achieving a decent compressive strength for reinforced fibre composites. Usually, three distributions of fibre reinforcement are followed during the manufacturing of continuous fibre reinforced composites, i.e. borders only, borders & centre and equidistant. Enhanced compressive resistance can be achieved for composites manufactured using the FDM method when the reinforcement distribution is equidistant. When continuous fibre is used as a reinforcement material, the reinforcement type and the reinforcement orientation play a significant role in the compressive strength of the composite manufactured using the FDM process.

Han et al. [159] manufactured a PEEK biocompatible carbon fibre reinforced composite suitable for orthopedic and dental applications. Both the compressive strength and the compressive modulus were analysed for the samples produced. It was also noted that PEEK reinforced carbon fibre composite (137 MPa) exhibited similar compressive strength compared to the pure PEEK material (138 MPa), although the modulus for pure PEEK was 2.7 GPa and for the composite, it was 3.5 GPa. This investigation suggested FDM printed PEEK and its composites for achieving better compressive properties. Kain et al. [160] investigated the effect of the infill orientation (0°, 15° crossed, 30° crossed, 45° crossed, 60° crossed, 75° crossed and 90° crossed) and the fibre content (15 and 25 wt %) on the compressive strength of the wood

Table 4
Impact strength of various FDM fabricated fibre composites.

Matrix	% of reinforcement	Notch condition	Max. Impact Strength	Remarks	Ref.
Nylon	34.3 vol% of GF	Notched	280.95 kJ/m^2	GF composites displayed the best impact performance compared to CF, leading to more brittle behaviour.	[148]
PA-12	10 wt% of CF	Unnotched	24.8 kJ/m^2	When the CF content increased to some extent such as 8 wt%, the effect of preventing crack propagation dominated the impact process, which contributed to the enhancement of the impact strength.	[124]
PLA	8.9 wt% of CF	Unnotched	38.7 kJ/m^2	No fibre pull-out was observed and only fibre breakage occurred on the sample after the impact test.	[137]
PP	15 wt% of SCF coated with 1 wt% of xGnPs	Notched	38.1 J/m	Increase in the impact strength was a result of the composites requiring more impact energy to pull out the xGnP–SCFs from the matrix owing to the rough surface of SCFs in the presence of xGnP.	[107]
PP	10 wt% of CF	Notched	40 kJ/m^2	Pure PP displayed plastic deformation on the fracture surface visible as elongated fibrils in large magnifications. The matrix of PP/CF10 appeared smooth and showed no plastic deformation due to brittle fracture.	[94]
PEEK	5 wt% of GF	Unnotched	30.2 kJ/m^2	Strong interfacial bonding among GF and PEEK compared to CF and PEEK was observed and this made it difficult to pull-out GF from PEEK.	[150]
Nylon	2 wt% aramid short fibres	–	0.637 MJ/m^2	Experimental results were interpreted with the Taguchi Technique	[151]
ASA	20 wt% of CF	Unnotched	18 kJ/m^2	The impact test resulted in a significant reduction of the absorbed energy (87%) by the 20 wt% CF composite as compared to the pure ASA.	[152]
PLA	20 wt% of CF	Notched	6.11 kJ/m^2	Increment of impact strength was observed when the CF content increased from 15 wt% to 20 wt%.	[153]

xGnPs: exfoliated graphene nanoplatelets, SCFs: Short Carbon Fibres; ASA: Acrylonitrile styrene acrylate.

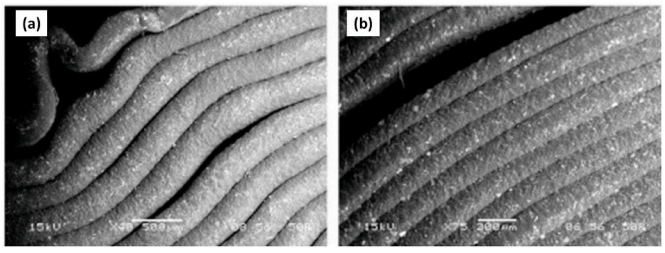

Fig. 13. SEM image of compression failed ABS composite (a) failure due to buckling and (b) de-bonding between layers, reproduced under the terms of the Creative Commons Attribution (CC-BY) license from Ref. [157].

fibre-reinforced PLA composite. The infill orientation had a direct effect on the compression strength of the PLA composite. The increase in the fibre content increased the compression strength of the composite. The maximum compression strength of 70 N/mm^2 was noted for 25 wt% of wood fibre composite printed with 15° infill orientation. In another study, Yang et al. [161] investigated the effect of the extrusion temperature on the compression strength of the FDM 3D unidirectional wood fibre-reinforced PLA composite. When the extrusion temperature was increased from 200 to 230 °C, the compressive strength of the composite was increased by 15%, while the other mechanical properties, i.e. the tensile and flexural properties, decreased. This was due to a decrease in the viscosity of the polymer at higher extrusion temperature, which tightly packed the fibre between the layers leading to an increase in the composite density that improved the compression strength.

Short carbon fibre reinforced PA6 composite was manufactured using FDM and polymer injection moulding (PIM) methods and the compression strength of the composite was investigated [162]. FDM printed composite showed a 4% reduction in compression strength compared to the injection moulded composite. However, 3D printed specimens exhibited higher rigidity than the injection moulded specimens. The compression modulus of the FDM printed fibre composite and injection moulded composite was 3931 MPa and 1950 MPa, respectively [162]. There is a dearth of studies reporting the compression modulus of FDM printed fibre composites. It is surprising to observe a high variation in the FDM printed composite modulus when compared to the injection moulded composite, although the FDM printed composite compression strength was 4% lower than the injection moulded composite. However, the rationale behind this phenomenon has not been properly addressed and further investigations into the compression modulus of FDM printed parts are warranted.

6. Thermal properties of FDM fibre composites fabricated through the FDM process

In addition to mechanical properties, FDM manufactured fibre composites were also investigated for their thermal behaviour, albeit the number of studies is few in number. Additive manufacturing involves repeated heating and cooling process, which could produce residual stress in the manufactured parts. The presence of residual stress may affect mechanical performance and also results in the bending of part and dimensional inaccuracies [163]. The thermal diffusivity and the thermal conductivity of carbon fibre reinforced PEEK composite fabricated from the FDM technique was compared with the composite fabricated by traditional casting [164]. Compared to composite fabricated with traditional casting, the composite fabricated with FDM 3D print technique showed a 25%–30% decrease in the thermal diffusivity and conductivity. The thermal diffusivity of the fibre composite was influenced by the fibre alignment formed during the melt flow. The PEEK carbon fibre composite's thermal diffusivity increased significantly with carbon fibre reinforcement. 30 wt% carbon fibre reinforcement exhibited high thermal diffusivity of 0.5 mm^2 and for 20 wt% reinforced composite it was 0.22 mm^2. Kaur et al. [156] studied the thermal properties of the FDM fabricated polymeric materials of PA618, PLA, and carbon fibre reinforced PLA. The thermal behaviour of these polymeric materials was analysed using differential scanning calorimetry (DSC) with the test temperature ranging from 25 to 270 °C at a heating rate of about 10 °C/min in a nitrogen atmosphere. 3D printed carbon-based PLA exhibited better thermal behaviour compared to the other polymeric materials under investigation. This is because the presence of carbon fibre accelerated the nucleation of PLA. Thermal variation in the printed PLA and carbon fibre reinforced PLA analysed in DSC at a heating rate of 10 °C/min is shown in Fig. 14. The printed PLA has a glass transition temperature of 57.07 °C, however, for the carbon fibre reinforced PLA, the glass transition temperature increased to 59.23 °C.

Composite printed at different build plate temperatures exhibited similar crystallisation peaks on the DSC test. These results concluded that the thermal variation in the printing environment does not influence the properties of the printed part and composite [162]. Yang et al. [161] reported that the increase in the extrusion temperature has a significant effect on the mechanical properties of wood-PLA composite. Composite fabricated at high extrusion temperature exhibited maximum tensile and flexural properties. The internal bonding strength was increased by up to 24% at 200 °C of extrusion temperature. Kain et al. [160] found similar thermal properties between wood fibre PLA composite and PLA material. It is because the thermal stability of the natural fibre composite largely depends on the thermoplastic polymers. Elsewhere, in a different study, the addition of carbon fibre to PA12 composite reduced the thermal degradation of the composite [124]. When increasing the fibre content, the onset of degradation temperature was also increased, fostering thermal stability in the composite. Carbon fibre reinforcement acted as a thermal stabiliser that protected the matrix through a shielding effect. The thermal conductivity along the print direction increased drastically to 278% compared to the pure PA12. In another study, De Toro et al. [165] investigated the thermal properties of 20 wt% carbon fibre reinforced PA composite, through DSC and thermogravimetry-differential thermal analysis. The composites showed a glass transition temperature of 50 °C, a melting point of 220 °C, and maximum degradation was observed at 450 °C.

Wang et al. [150] investigated the thermal stability of PEEK composites reinforced with short carbon fibre (average length of 205 μm) and glass fibre (average length of 96 μm). Composites were manufactured with varying fibre reinforcements of 5, 10, and 15 wt%. Glass fibre composites exhibited better thermal stability than the carbon fibre composites due to enhanced interfacial bonding. A minimum weight loss of 43% was noted for 10 wt% glass fibre composite, while for 10 wt% carbon fibre composite the same was 47%. An increase in the melting point, thermal decomposition temperature, and crystallisation temperature was noted on the composites when increasing the fibre content. Similar results were reported by Vinyas et al. [166] for 30 wt% glass fibre reinforced PLA composite. The degradation temperature of the glass fibre PLA composite was 442 °C, which was 25% higher than that of the pure PLA. From these results, it is identified that fibre reinforcement in FDM-printed polymer could provide enhanced thermal stability. The fibre reinforcement limits the movement of the polymer molecular chains leading to higher thermal stability than the pure polymer.

Li et al. [112] investigated the dynamic mechanical properties of FDM printed continuous carbon fibre PLA composites. The composites were made with carbon fibre and with fibre having a modified surface. Surface modification was performed using aqueous solution containing methylene dichloride and PLA particles. The glass transition temperature and the storage modulus of modified carbon fibre composite were higher than the pure and original carbon fibre composite. The storage modulus of the modified carbon fibre reinforced PLA composites was 3.25 GPa, which was 166% and 351% higher than the pure PLA and the original carbon fibre reinforced composites, respectively. In another study, Zhang et al. [58] examined the influence of the raster angle on the dynamic mechanical properties of FDM-printed aluminium fibre composites. Composites were printed at varying raster orientations of 0°, 90°, 45°, 0°/90° and ±45° with PLA/aluminium fibre composite filament having 6.95 wt% of aluminium fibre. The increased stiffness due to the addition of aluminium fibre increased the storage modulus of the composites. A maximum storage modulus of 3.87 GPa was observed for the composite printed at 0° raster angle, however, a maximum glass transition temperature of 72.34 °C was noted for the composite printed at 90° raster angle. Nevertheless, it was found that literature reporting the influence of the FDM parameter on the thermal properties of printed composites is limited. Investigating the influence of FDM parameters on the thermal properties of FDM-based fibre composites could lead to interesting new findings.

7. Summary and future research scopes

The present review article summarises the performance of the fibre-reinforced composites manufactured through AM, in particular the FDM method. In recent years, the FDM process has achieved significant improvement in developing fibre composites. The review investigated both the short and continuous fibre-reinforced composites. Most of the literature is concentrated on the effect of carbon fibre reinforcement in FDM fabricated composites and future research should be focused on different synthetic and natural fibre reinforcements. In FDM, the effect of natural fibre is studied by only a few researches, which provides an impetus for the development of natural fibre composites through FDM. The fibre and matrix interaction could be increased through fibre

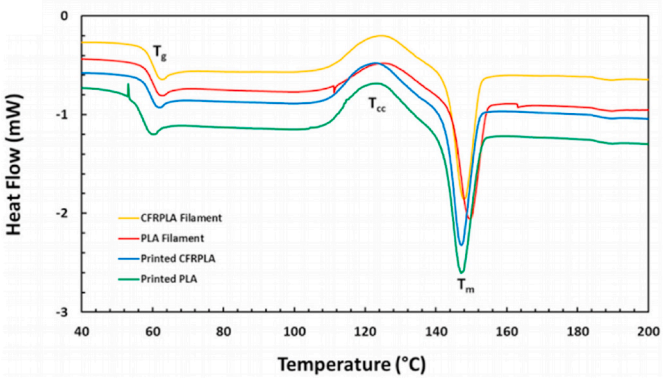

Fig. 14. Thermal variation in the printed PLA and carbon fibre reinforced PLA (CFRPLA), reproduced with permission from Refs. [156]. (T_g = glass transition temperature; T_{cc} = recrystallisation temperature; T_m = melting temperature).

treatment and other processing methods that can also aid in avoiding the formation of voids. The void formation was found to be a more common printing defect in FDM of fibre composites. Variation in fibre content, fibre orientation, and fibre-matrix bonding was found to be the crucial parameters deciding the part performance. The increase in fibre reinforcement content and fibre length contributed to increased strength. Regarding mechanical performance, although a number of literatures reported the tensile characteristics, only a limited study examined the flexural behaviour of the composite while there are even fewer studies relating to the compression strength and impact strength. To understand the AM fibre composites' strength, the mechanical properties should be investigated in more detail concerning fracture mechanics. Understanding of FDM process parameters is important to enhance the part performance. It is therefore essential to optimise the FDM process parameters. Modelling should be developed to comprehend the significance of the parameters on part performance. Moreover, to establish FDM as a viable process for developing fibre composites, research on the development of a modelling tool to predict the process and its consequences are important. Furthermore, the rheological properties of polymer matrix/filament and morphology should be studied when reinforced with fibres. Only a few thermoset based 3D printed fibre composites performance were reported and development in this area can enable high-performance composites. In AM, composites' defect formation chances are high leading to reduced strength. Hence, investigating the defect formation mechanism could reduce the possibility of the defect and consequently increase the performance properties. More detailed and fundamental research on FDM-based fibre composites' performance is required to warrant their foray into modern applications. The FDM method is found to be the most potential and promising method for the development of fibre composites, which can reduce the composite processing time and cost.

CRediT authorship contribution statement

Vigneshwaran Shanmugam: Conceptualization, Writing - original draft, Writing - review & editing. **Deepak Joel Johnson Rajendran:** Writing - original draft, Writing - review & editing. **Karthik Babu:** Writing - original draft, Writing - review & editing. **Sundarakannan Rajendran:** Writing - original draft, Writing - review & editing. **Arumugaprabu Veerasimman:** Writing - original draft, Writing - review & editing. **Uthayakumar Marimuthu:** Supervision, Writing - review & editing. **Sunpreet Singh:** Writing - original draft, Writing - review & editing. **Oisik Das:** Conceptualization, Writing - original draft, Writing - review & editing. **Rasoul Esmaeely Neisiany:** Conceptualization, Writing - original draft, Writing - review & editing. **Mikael S. Hedenqvist:** Writing - review & editing. **Filippo Berto:** Writing - review & editing. **Seeram Ramakrishna:** Supervision, Writing - review & editing.

Declaration of competing interest

The authors declare that they have no known competing financial interests or personal relationships that could have appeared to influence the work reported in this paper.

References

[1] T.J. Snyder, M. Andrews, M. Weislogel, P. Moeck, J. Stone-Sundberg, D. Birkes, et al., 3D systems' technology overview and new applications in manufacturing, engineering, science, and education, 3D Print. Addit. Manuf. 1 (2014) 169–176, https://doi.org/10.1089/3dp.2014.1502.

[2] G.D. Goh, Y.L. Yap, H.K.J. Tan, S.L. Sing, G.L. Goh, W.Y. Yeong, Process–structure–properties in polymer additive manufacturing via material extrusion: a review, Crit. Rev. Solid State Mater. Sci. 1–21 (2019), https://doi.org/10.1080/10408436.2018.1549977.

[3] V. Shanmugam, O. Das, R.E. Neisiany, K. Babu, S. Singh, M.S. Hedenqvist, F. Berto, S. Ramakrishna, Polymer Recycling in Additive Manufacturing: an Opportunity for the Circular Economy, Mater. Circ. Econ 2 (11) (2020), https://doi.org/10.1007/s42824-020-00012-0.

[4] J. Gardan, Additive manufacturing technologies: state of the art and trends, Int. J. Prod. Res. 54 (2016) 3118–3132, https://doi.org/10.1080/00207543.2015.1115909.

[5] B. Wendel, D. Rietzel, F. Kühnlein, R. Feulner, G. Hülder, E. Schmachtenberg, Additive processing of polymers, Macromol. Mater. Eng. 293 (2008) 799–809, https://doi.org/10.1002/mame.200800121.

[6] M. Vaezi, S. Chianrabutra, B. Mellor, S. Yang, Multiple material additive manufacturing - Part 1: a review, Virtual Phys. Prototyp. 8 (2013) 19–50, https://doi.org/10.1080/17452759.2013.778175.

[7] Z.X. Khoo, J.E.M. Teoh, Y. Liu, C.K. Chua, S. Yang, J. An, et al., 3D printing of smart materials: a review on recent progresses in 4D printing, Virtual Phys. Prototyp. 10 (2015) 103–122, https://doi.org/10.1080/17452759.2015.1097054.

[8] V. Shanmugam, O. Das, K. Babu, U. Marimuthu, A. Veerasimman, D.J. Johnson, R.E. Neisiany, M.S. Hedenqvist, S. Ramakrishna, F. Berto, Fatigue behaviour of FDM-3D printed polymers, polymeric composites and architected cellular materials, Int. J. Fatigue 143 (2021) 106007, https://doi.org/10.1016/j.ijfatigue.2020.106007.

[9] R.E. Neisiany, S.N. Khorasani, M. Naeimirad, J.K.Y. Lee, S. Ramakrishna, Improving mechanical properties of carbon/epoxy composite by incorporating functionalized electrospun polyacrylonitrile nanofibers, Macromol. Mater. Eng. 302 (2017) 1600551, https://doi.org/10.1002/mame.201600551.

[10] S.M.F. Kabir, K. Mathur, A.F.M. Seyam, A critical review on 3D printed continuous fibre-reinforced composites: history, mechanism, materials and properties, Compos. Struct. 232 (2020) 111476, https://doi.org/10.1016/j.compstruct.2019.111476.

[11] T.N.A.T. Rahim, A.M. Abdullah, H. Md Akil, Recent developments in fused deposition modeling-based 3D printing of polymers and their composites, Polym. Rev. 59 (2019) 589–624, https://doi.org/10.1080/15583724.2019.1597883.

[12] A.S. Mangat, S. Singh, M. Gupta, R. Sharma, Experimental investigations on natural fibre embedded additive manufacturing-based biodegradable structures for biomedical applications, Rapid Prototyp. J. 24 (2018) 1221–1234, https://doi.org/10.1108/RPJ-08-2017-0162.

[13] T.D. Ngo, A. Kashani, G. Imbalzano, K.T.Q. Nguyen, D. Hui, Additive manufacturing (3D printing): a review of materials, methods, applications and challenges, Compos. B Eng. 143 (2018) 172–196, https://doi.org/10.1016/j.compositesb.2018.02.012.

[14] A. Nasirov, I. Fidan, Prediction of mechanical properties of fused filament fabricated structures via asymptotic homogenization, Mech. Mater. 145 (2020), https://doi.org/10.1016/j.mechmat.2020.103372.

[15] C. Wendt, A.P. Valerga, O. Droste, M. Batista, M. Marcos, FEM based evaluation of Fused Layer Modelling monolayers in tensile testing, Procedia Manufact. 13 (2017) 916–923, https://doi.org/10.1016/j.promfg.2017.09.160.

[16] E. Cuan-Urquizo, J.I. Espinoza-Camacho, A. Álvarez-Trejo, E. Uribe, C.D. Treviño-Quintanilla, S.E. Crespo-Sánchez, et al., Elastic response of lattice arc structures fabricated using curved-layered fused deposition modeling, Mech. Adv. Mater. Struct. (2019), https://doi.org/10.1080/15376494.2019.1682728.

[17] S.H. Ahn, M. Montero, D. Odell, S. Roundy, P.K. Wright, Anisotropic material properties of fused deposition modeling ABS, Rapid Prototyp. J. 8 (2002) 248–257, https://doi.org/10.1108/13552540210441166.

[18] N. Mohan, P. Senthil, S. Vinodh, N. Jayanth, A review on composite materials and process parameters optimisation for the fused deposition modelling process, Virtual Phys. Prototyp. 12 (2017) 47–59, https://doi.org/10.1080/17452759.2016.1274490.

[19] W. Zhong, F. Li, Z. Zhang, L. Song, Z. Li, Short fibre reinforced composites for fused deposition modeling, Mater. Sci. Eng. 301 (2001) 125–130, https://doi.org/10.1016/S0921-5093(00)01810-4.

[20] L.J. Love, V. Kunc, O. Rios, C.E. Duty, A.M. Elliott, B.K. Post, et al., The importance of carbon fibre to polymer additive manufacturing, J. Mater. Res. 29 (2014) 1893–1898, https://doi.org/10.1557/jmr.2014.212.

[21] T. Hofstätter, D.B. Pedersen, G. Tosello, H.N. Hansen, State-of-the-art of fibre-reinforced polymers in additive manufacturing technologies, J. Reinforc. Plast. Compos. 36 (2017) 1061–1073, https://doi.org/10.1177/0731684417695648.

[22] Y. Nakagawa, K ichiro Mori, T. Maeno, 3D printing of carbon fibre-reinforced plastic parts, Int. J. Adv. Manuf. Technol. 91 (2017) 2811–2817, https://doi.org/10.1007/s00170-016-9891-7.

[23] S. Garzon-Hernandez, D. Garcia-Gonzalez, A. Jérusalem, A. Arias, Design of FDM 3D printed polymers: an experimental-modelling methodology for the prediction of mechanical properties, Mater. Des. 188 (2020), https://doi.org/10.1016/j.matdes.2019.108414.

[24] H. Prüß, T. Vietor, Design for fibre-reinforced additive manufacturing, J. Mech. Design, Trans. ASME 137 (2015), https://doi.org/10.1115/1.4030993, 111409-1-111409–7.

[25] J. Wang, H. Xie, Z. Weng, T. Senthil, L. Wu, A novel approach to improve mechanical properties of parts fabricated by fused deposition modeling, Mater. Des. 105 (2016) 152–159, https://doi.org/10.1016/j.matdes.2016.05.078.

[26] S.M.J. Razavi, R.E. Neisiany, S.N. Khorasani, S. Ramakrishna, F. Berto, Effect of neat and reinforced polyacrylonitrile nanofibers incorporation on interlaminar fracture toughness of carbon/epoxy composite, Theoret. Appl. Mechanics Lett. 8 (2018) 126–131, https://doi.org/10.1016/j.taml.2018.02.008.

[27] R.E. Neisiany, S.N. Khorasani, J.K.Y. Lee, M. Naeimirad, S. Ramakrishna, Interfacial toughening of carbon/epoxy composite by incorporating styrene acrylonitrile nanofibers, Theor. Appl. Fract. Mech. 95 (2018) 242–247, https://doi.org/10.1016/j.tafmec.2018.03.006.

[28] S. Wickramasinghe, T. Do, P. Tran, FDM-based 3D printing of polymer and associated composite: a review on mechanical properties, defects and treatments, Polymers 12 (2020) 1529, https://doi.org/10.3390/polym12071529.

[29] G.D. Goh, Y.L. Yap, S. Agarwala, W.Y. Yeong, Recent progress in additive manufacturing of fibre reinforced polymer composite, Adv. Mater. Technol. 4 (2019) 1800271, https://doi.org/10.1002/admt.201800271.

[30] N. van de Werken, H. Tekinalp, P. Khanbolouki, S. Ozcan, A. Williams, M. Tehrani, Additively manufactured carbon fibre-reinforced composites: state of the art and perspective, Additive Manufac. 31 (2020) 100962, https://doi.org/10.1016/j.addma.2019.100962.

[31] V. Wong, Aldo Hernandez, A Review of Additive Manufacturing, International Scholarly Research Notices, 2012, https://doi.org/10.5402/2012/208760. Article ID 208760.

[32] L. Yang, K. Hsu, B. Baughman, D. Godfrey, F. Medina, M. Menon, et al., Additive Manufacturing of Metals: the Technology, Materials, Design and Production, Springer International Publishing, 2017, https://doi.org/10.1007/978-3-319-55128-9.

[33] W. Zha, S. Anand, Geometric approaches to input file modification for part quality improvement in additive manufacturing, J. Manuf. Process. 20 (2015) 465–477, https://doi.org/10.1016/j.jmapro.2015.06.021.

[34] A. Gebhardt, Understanding Additive Manufacturing Rapid Prototyping - Rapid Tooling - Rapid Manufacturing, Carl Hanser, München, 2012, p. 591, https://doi.org/10.3139/9783446431621.

[35] S. Hällgren, L. Pejryd, J. Ekengren, 3D data export for additive manufacturing-improving geometric accuracy, in: Procedia CIRP, vol. 50, Elsevier B.V., 2016, pp. 518–523, https://doi.org/10.1016/j.procir.2016.05.046.

[36] I. Gibson, D. Rosen, B. Stucker, I. Gibson, D. Rosen, B. Stucker, Software Issues for Additive Manufacturing. Additive Manufacturing Technologies, Springer, New York, 2015, pp. 351–374, https://doi.org/10.1007/978-1-4939-2113-3_15.

[37] Y an Jin, Y. He, J. Fu, zhong, Support generation for additive manufacturing based on sliced data, Int. J. Adv. Manuf. Technol. 80 (2015) 2041–2052, https://doi.org/10.1007/s00170-015-7190-3.

[38] R. Vaidya, S. Anand, Image processing assisted tools for pre- and post-processing operations in additive manufacturing, Procedia Manufact. 5 (2016) 958–973, https://doi.org/10.1016/j.promfg.2016.08.084.

[39] C.K. Chua, K.F. Leong, 3D Printing and Additive Manufacturing: Principles and Applications: the 5th Edition of Rapid Prototyping: Principles and Applications, World Scientific Publishing Co., 2017, https://doi.org/10.1142/10200.

[40] M. Revilla-León, L. Ceballos, I. Martínez-Klemm, M. Özcan, Discrepancy of complete-arch titanium frameworks manufactured using selective laser melting and electron beam melting additive manufacturing technologies, J. Prosthet. Dent 120 (2018) 942–947, https://doi.org/10.1016/j.prosdent.2018.02.010.

[41] S. Chung, S.E. Song, Y.T. Cho, Effective software solutions for 4D printing: a review and proposal, Int. J. Prec. Eng. Manufact. Green Technol. 4 (2017) 359–371, https://doi.org/10.1007/s40684-017-0041-y.

[42] L. Rebaioli, P. Magnoni, I. Fassi, N. Pedrocchi, L. Molinari Tosatti, Process parameters tuning and online re-slicing for robotized additive manufacturing of big plastic objects, Robot. Comput. Integrated Manuf. 55 (2019) 55–64, https://doi.org/10.1016/j.rcim.2018.07.012.

[43] S. Sikder, A. Barari, H.A. Kishawy, Effect of Adaptive Slicing on Surface Integrity in Additive Manufacturing, ASME International, 2014, https://doi.org/10.1115/detc2014-35559.

[44] J.C. Steuben, A.P. Iliopoulos, J.G. Michopoulos, Implicit slicing for functionally tailored additive manufacturing, CAD Comp. Aided Design 77 (2016) 107–119, https://doi.org/10.1016/j.cad.2016.04.003.

[45] J.P. Kruth, M.C. Leu, T. Nakagawa, Progress in additive manufacturing and rapid prototyping, CIRP Ann. - Manuf. Technol. 47 (1998) 525–540, https://doi.org/10.1016/S0007-8506(07)63240-5.

[46] S. Lim, R.A. Buswell, T.T. Le, S.A. Austin, A.G.F. Gibb, T. Thorpe, Developments in construction-scale additive manufacturing processes, Autom. ConStruct. 21 (2012) 262–268, https://doi.org/10.1016/j.autcon.2011.06.010.

[47] A.C. Brown, D. De Beer, Development of a stereolithography (STL) slicing and G-code generation algorithm for an entry level 3-D printer, in: IEEE AFRICON Conference, Institute of Electrical and Electronics Engineers Inc, 2013, https://doi.org/10.1109/AFRCON.2013.6757836.

[48] I. Gibson, D. Rosen, B. Stucker, Additive Manufacturing Technologies: 3D Printing, Rapid Prototyping, and Direct Digital Manufacturing, second ed., Springer, New York, 2015 https://doi.org/10.1007/978-1-4939-2113-3.

[49] N.N. Kumbhar, A.V. Mulay, Post processing methods used to improve surface finish of products which are manufactured by additive manufacturing technologies: a review, J. Inst. Eng.: Series C 99 (2018) 481–487, https://doi.org/10.1007/s40032-016-0340-z.

[50] S. Cheruvathur, E.A. Lass, C.E. Campbell, Additive manufacturing of 17-4 PH stainless steel: post-processing heat treatment to achieve uniform reproducible microstructure, J. Occup. Med. 68 (2016) 930–942, https://doi.org/10.1007/s11837-015-1754-4.

[51] A. Levy, A. Miriyev, N. Sridharan, T. Han, E. Tuval, S.S. Babu, et al., Ultrasonic additive manufacturing of steel: method, post-processing treatments and properties, J. Mater. Process. Technol. 256 (2018) 183–189, https://doi.org/10.1016/j.jmatprotec.2018.02.001.

[52] M. Domingo-Espin, J.M. Puigoriol-Forcada, A.A. Garcia-Granada, J. Llumà, S. Borros, G. Reyes, Mechanical property characterization and simulation of fused deposition modeling Polycarbonate parts, Mater. Des. 83 (2015) 670–677, https://doi.org/10.1016/j.matdes.2015.06.074.

[53] J. Martínez, J.L. Diéguez, E. Ares, A. Pereira, P. Hernández, J.A. Pérez, Comparative between FEM models for FDM parts and their approach to a real mechanical behaviour, in: Procedia Engineering, vol. 63, Elsevier Ltd, 2013, pp. 878–884, https://doi.org/10.1016/j.proeng.2013.08.230.

[54] Nováková-Marcinčinová Ľ, I. Kurić, Basic and Advanced Materials for Fused Deposition Modeling Rapid Prototyping Technology, 2012.

[55] H. Wu, W.P. Fahy, S. Kim, H. Kim, N. Zhao, L. Pilato, et al., Recent developments in polymers/polymer nanocomposites for additive manufacturing, Prog. Mater. Sci. 111 (2020), https://doi.org/10.1016/j.pmatsci.2020.100638.

[56] J. Justo, L. Távara, L. García-Guzmán, F. París, Characterization of 3D printed long fibre reinforced composites, Compos. Struct. 185 (2018) 537–548, https://doi.org/10.1016/j.compstruct.2017.11.052.

[57] A.P. Valerga, M. Batista, R. Puyana, A. Sambruno, C. Wendt, M. Marcos, Preliminary study of PLA wire colour effects on geometric characteristics of parts manufactured by FDM, Procedia Manufact. 13 (2017) 924–931, https://doi.org/10.1016/j.promfg.2017.09.161.

[58] X. Zhang, L. Chen, T. Mulholland, T.A. Osswald, Effects of raster angle on the mechanical properties of PLA and Al/PLA composite part produced by fused deposition modeling, Polym. Adv. Technol. 30 (2019) 2122–2135, https://doi.org/10.1002/pat.4645.

[59] D. Jiang, D.E. Smith, Anisotropic mechanical properties of oriented carbon fibre filled polymer composites produced with fused filament fabrication, Additive Manufac. 18 (2017) 84–94, https://doi.org/10.1016/j.addma.2017.08.006.

[60] O.A. Mohamed, S.H. Masood, J.L. Bhowmik, Optimization of fused deposition modeling process parameters: a review of current research and future prospects, Adv. Manufact. 3 (2015) 42–53, https://doi.org/10.1007/s40436-014-0097-7.

[61] R. Anitha, S. Arunachalam, P. Radhakrishnan, Critical parameters influencing the quality of prototypes in fused deposition modelling, J. Mater. Process. Technol. 118 (2001) 385–388, https://doi.org/10.1016/S0924-0136(01)00980-3. Elsevier.

[62] T.R.D.R.V. Nancharaiah, An experimental investigation on surface quality and dimensional accuracy of FDM components, Int. J. Emerg. Technol. 1 (2010) 106–111.

[63] R.N.M.M. Daniel Horvath, Improvement of surface roughness on ABS 400 polymer using design of experiments (DOE) | Scientific.Net, Mater. Sci. Forum 561 (2007) 2389–2392.

[64] C.C. Wang, T.W. Lin, S.S. Hu, Optimizing the rapid prototyping process by integrating the Taguchi method with the Gray relational analysis, Rapid Prototyp. J. 13 (2007) 304–315, https://doi.org/10.1108/13552540710824814.

[65] O.S. Carneiro, A.F. Silva, R. Gomes, Fused deposition modeling with polypropylene, Mater. Des. 83 (2015) 768–776, https://doi.org/10.1016/j.matdes.2015.06.053.

[66] C. Bellehumeur, L. Li, Q. Sun, P. Gu, Modeling of bond formation between polymer filaments in the fused deposition modeling process, J. Manuf. Process. 6 (2004) 170–178, https://doi.org/10.1016/S1526-6125(04)70071-7.

[67] J.C. Riddick, M.A. Haile, R Von Wahlde, D.P. Cole, O. Bamiduro, T.E. Johnson, Fractographic analysis of tensile failure of acrylonitrile-butadiene-styrene fabricated by fused deposition modeling, Additive Manufac. 11 (2016) 49–59, https://doi.org/10.1016/j.addma.2016.03.007.

[68] A. García-Domínguez, J. Claver, M.A. Sebastián, Methodology for the optimization of work pieces for additive manufacturing by 3D printing, Procedia Manufact. 13 (2017) 910–915, https://doi.org/10.1016/j.promfg.2017.09.158.

[69] K. Gnanasekaran, T. Heijmans, S. van Bennekom, H. Woldhuis, S. Wijnia, G. de With, et al., 3D printing of CNT- and graphene-based conductive polymer nanocomposites by fused deposition modeling, Appl. Mater. Today 9 (2017) 21–28, https://doi.org/10.1016/j.apmt.2017.04.003.

[70] H.L. Tekinalp, V. Kunc, G.M. Velez-Garcia, C.E. Duty, L.J. Love, A.K. Naskar, et al., Highly oriented carbon fibre-polymer composites via additive manufacturing, Compos. Sci. Technol. 105 (2014) 144–150, https://doi.org/10.1016/j.compscitech.2014.10.009.

[71] S.J. Kalita, S. Bose, H.L. Hosick, A. Bandyopadhyay, Development of controlled porosity polymer-ceramic composite scaffolds via fused deposition modeling, Mater. Sci. Eng. C 23 (2003) 611–620, https://doi.org/10.1016/S0928-4931(03)00052-3.

[72] S. Berretta, R. Davies, Y.T. Shyng, Y. Wang, O. Ghita, Fused Deposition Modelling of high temperature polymers: exploring CNT PEEK composites, Polym. Test. 63 (2017) 251–262, https://doi.org/10.1016/j.polymertesting.2017.08.024.

[73] S. Ding, B. Zou, P. Wang, H. Ding, Effects of nozzle temperature and building orientation on mechanical properties and microstructure of PEEK and PEI printed by 3D-FDM, Polym. Test. 78 (2019) 105948, https://doi.org/10.1016/j.polymertesting.2019.105948.

[74] B. Brenken, E. Barocio, A. Favaloro, V. Kunc, R.B. Pipes, Fused filament fabrication of fibre-reinforced polymers: a review, Additive Manufac. 21 (2018) 1–16, https://doi.org/10.1016/j.addma.2018.01.002.

[75] G. Alaimo, S. Marconi, L. Costato, F. Auricchio, Influence of meso-structure and chemical composition on FDM 3D-printed parts, Compos. B Eng. 113 (2017) 371–380, https://doi.org/10.1016/j.compositesb.2017.01.019.

[76] N. Aliheidari, J. Christ, R. Tripuraneni, S. Nadimpalli, A. Ameli, Interlayer adhesion and fracture resistance of polymers printed through melt extrusion additive manufacturing process, Mater. Des. 156 (2018) 351–361, https://doi.org/10.1016/j.matdes.2018.07.001.

[77] K.R. Hart, R.M. Dunn, J.M. Sietins, C.M. Hofmeister Mock, M.E. Mackay, E. D. Wetzel, Increased fracture toughness of additively manufactured amorphous thermoplastics via thermal annealing, Polymer 144 (2018) 192–204, https://doi.org/10.1016/j.polymer.2018.04.024.

[78] M. Jin, R. Giesa, C. Neuber, H. Schmidt, Filament materials screening for FDM 3D printing by means of injection-molded short rods, Macromol. Mater. Eng. 303 (2018) 1800507, https://doi.org/10.1002/mame.201800507.

[79] B.N. Turner, S.A. Gold, A review of melt extrusion additive manufacturing processes: II. Materials, dimensional accuracy, and surface roughness, Rapid Prototyp. J. 21 (2015) 250–261, https://doi.org/10.1108/RPJ-02-2013-0017.

[80] B.N. Turner, R. Strong, S.A. Gold, A review of melt extrusion additive manufacturing processes: I. Process design and modeling, Rapid Prototyp. J. 20 (2014) 192–204, https://doi.org/10.1108/RPJ-01-2013-0012.

[81] O. Pokluda, C.T. Bellehumeur, J. Vlachopoulos, Modification of Frenkel's model for sintering, AIChE J. 43 (1997) 3253–3256, https://doi.org/10.1002/aic.690431213.

[82] Q. Sun, G.M. Rizvi, C.T. Bellehumeur, P. Gu, Effect of processing conditions on the bonding quality of FDM polymer filaments, Rapid Prototyp. J. 14 (2008) 72–80, https://doi.org/10.1108/13552540810862028.

[83] L. Li, Q. Sun, C. Bellehumeur, P. Gu, Investigation of bond formation in FDM process 400, in: International Solid Freeform Fabrication Symposium., 2002, 2002, https://doi.org/10.26153/TSW/4500.

[84] A.R. Torrado, C.M. Shemelya, J.D. English, Y. Lin, R.B. Wicker, D.A. Roberson, Characterizing the effect of additives to ABS on the mechanical property anisotropy of specimens fabricated by material extrusion 3D printing, Additive Manufac. 6 (2015) 16–29, https://doi.org/10.1016/j.addma.2015.02.001.

[85] Modeling the fracture strength between fused-deposition extruded roads 16, in: J. P. Thomas, J.F. Rodríguez (Eds.), International Solid Freeform Fabrication Symposium, 2000, pp. 17–23.

[86] S. Costa, F. Duarte, J. A, Using MATLAB to compute heat transfer in free form extrusion, in: MATLAB - A Ubiquitous Tool for the Practical Engineer, InTech, 2011, https://doi.org/10.5772/23512.

[87] J. Rodriguez, J. Thomas, J. Renaud, Maximizing the strength of fused-deposition ABS plastic parts, in: International Solid Freeform Fabrication Symposium, 1999, 1999.

[88] N. Aliheidari, R. Tripuraneni, A. Ameli, S. Nadimpalli, Fracture resistance measurement of fused deposition modeling 3D printed polymers, Polym. Test. 60 (2017) 94–101, https://doi.org/10.1016/j.polymertesting.2017.03.016.

[89] D. Young, N. Wetmore, M. Czabaj, Interlayer fracture toughness of additively manufactured unreinforced and carbon-fibre-reinforced acrylonitrile butadiene styrene, Additive Manufac. 22 (2018) 508–515, https://doi.org/10.1016/j.addma.2018.02.023.

[90] Q. Tarrés, J.K. Melbø, M. Delgado-Aguilar, F.X. Espinach, P. Mutjé, G. Chinga-Carrasco, Bio-polyethylene reinforced with thermomechanical pulp fibres: mechanical and micromechanical characterization and its application in 3D-printing by fused deposition modelling, Compos. B Eng. 153 (2018) 70–77, https://doi.org/10.1016/j.compositesb.2018.07.009.

[91] N.P. Levenhagen, M.D. Dadmun, Interlayer diffusion of surface segregating additives to improve the isotropy of fused deposition modeling products, Polymer 152 (2018) 35–41, https://doi.org/10.1016/j.polymer.2018.01.031.

[92] R.A. Wach, P. Wolszczak, A. Adamus-Wlodarczyk, Enhancement of mechanical properties of FDM-PLA parts via thermal annealing, Macromol. Mater. Eng. 303 (2018) 1800169, https://doi.org/10.1002/mame.201800169.

[93] T. Mulholland, S. Goris, J. Boxleitner, T. Osswald, N. Rudolph, Process-induced fibre orientation in fused filament fabrication, J. Compos. Sci. 2 (2018) 45, https://doi.org/10.3390/jcs2030045.

[94] M. Spoerk, C. Savandaiah, F. Arbeiter, G. Traxler, L. Cardon, C. Holzer, et al., Anisotropic properties of oriented short carbon fibre filled polypropylene parts fabricated by extrusion-based additive manufacturing, Compos. Appl. Sci. Manuf. 113 (2018) 95–104, https://doi.org/10.1016/j.compositesa.2018.06.018.

[95] T. Hofstätter, I.W. Gutmann, T. Koch, D.B. Pedersen, G. Tosello, G. Heinz, et al., Distribution and orientation of carbon fibres in polylactic acid parts produced by fused deposition modeling, in: ASPE Summer Topical Meeting 2016, The American Society for Precision Engineering, 2016.

[96] B.P. Heller, D.E. Smith, D.A. Jack, Effects of extrudate swell and nozzle geometry on fibre orientation in Fused Filament Fabrication nozzle flow, Additive Manufac. 12 (2016) 252–264, https://doi.org/10.1016/j.addma.2016.06.005.

[97] H. Zhang, D. Yang, Y. Sheng, Performance-driven 3D printing of continuous curved carbon fibre reinforced polymer composites: a preliminary numerical study, Compos. B Eng. 151 (2018) 256–264, https://doi.org/10.1016/j.compositesb.2018.06.017.

[98] A.A. Safonov, 3D topology optimization of continuous fibre-reinforced structures via natural evolution method, Compos. Struct. 215 (2019) 289–297, https://doi.org/10.1016/j.compstruct.2019.02.063.

[99] B.P. Heller, D.E. Smith, D.A. Jack, Effect of extrudate swell, nozzle shape, and convergence zone on fibre orientation in fused deposition modeling nozzle flow, in: Proceedings of the Solid Freeform Fabrication, Austin, TX, USA, 2015, pp. 1220–1236.

[100] M. Mohammadizadeh, A. Imeri, I. Fidan, M. Elkelany, 3D printed fibre reinforced polymer composites - structural analysis, Compos. B Eng. 175 (2019) 107112, https://doi.org/10.1016/j.compositesb.2019.107112.

[101] E.A. Papon, A. Haque, Fracture toughness of additively manufactured carbon fibre reinforced composites, Additive Manufac. 26 (2019) 41–52, https://doi.org/10.1016/j.addma.2018.12.010.

[102] A.D. Pertuz, S. Díaz-Cardona, O.A. González-Estrada, Static and fatigue behaviour of continuous fibre reinforced thermoplastic composites manufactured by fused deposition modelling technique, Int. J. Fatig. 130 (2020) 105275, https://doi.org/10.1016/j.ijfatigue.2019.105275.

[103] P. Parandoush, L. Tucker, C. Zhou, D. Lin, Laser assisted additive manufacturing of continuous fibre reinforced thermoplastic composites, Mater. Des. 131 (2017) 186–195, https://doi.org/10.1016/j.matdes.2017.06.013.

[104] T. Liu, X. Tian, M. Zhang, D. Abliz, D. Li, G. Ziegmann, Interfacial performance and fracture patterns of 3D printed continuous carbon fibre with sizing reinforced PA6 composites, Compos. Appl. Sci. Manuf. 114 (2018) 368–376, https://doi.org/10.1016/j.compositesa.2018.09.001.

[105] G. Sodeifian, S. Ghaseminejad, A.A. Yousefi, Preparation of polypropylene/short glass fibre composite as Fused Deposition Modeling (FDM) filament, Results Phys. 12 (2019) 205–222, https://doi.org/10.1016/j.rinp.2018.11.065.

[106] X. Yao, C. Luan, D. Zhang, L. Lan, J. Fu, Evaluation of carbon fibre-embedded 3D printed structures for strengthening and structural-health monitoring, Mater. Des. 114 (2017) 424–432, https://doi.org/10.1016/j.matdes.2016.10.078.

[107] A. Ashori, S. Menbari, R. Bahrami, Mechanical and thermo-mechanical properties of short carbon fibre reinforced polypropylene composites using exfoliated graphene nanoplatelets coating, J. Ind. Eng. Chem. 38 (2016) 37–42, https://doi.org/10.1016/j.jiec.2016.04.003.

[108] Z. Liu, Q. Lei, S. Xing, Mechanical characteristics of wood, ceramic, metal and carbon fibre-based PLA composites fabricated by FDM, J. Mater. Res. Technol. 8 (2019) 3743–3753, https://doi.org/10.1016/j.jmrt.2019.06.034.

[109] A. Le Duigou, M. Castro, R. Bevan, N. Martin, 3D printing of wood fibre biocomposites: from mechanical to actuation functionality, Mater. Des. 96 (2016) 106–114, https://doi.org/10.1016/j.matdes.2016.02.018.

[110] P. Bettini, G. Alitta, G. Sala, L. Di Landro, Fused deposition technique for continuous fibre reinforced thermoplastic, J. Mater. Eng. Perform. 26 (2017) 843–848, https://doi.org/10.1007/s11665-016-2459-8.

[111] F. Ning, W. Cong, Y. Hu, H. Wang, Additive manufacturing of carbon fibre-reinforced plastic composites using fused deposition modeling: effects of process parameters on tensile properties, J. Compos. Mater. 51 (2017) 451–462, https://doi.org/10.1177/0021998316646169.

[112] N. Li, Y. Li, S. Liu, Rapid prototyping of continuous carbon fibre reinforced polylactic acid composites by 3D printing, J. Mater. Process. Technol. 238 (2016) 218–225, https://doi.org/10.1016/j.jmatprotec.2016.07.025.

[113] W. Zhang, C. Cotton, J. Sun, D. Heider, B. Gu, B. Sun, et al., Interfacial bonding strength of short carbon fibre/acrylonitrile-butadiene-styrene composites fabricated by fused deposition modeling, Compos. B Eng. 137 (2018) 51–59, https://doi.org/10.1016/j.compositesb.2017.11.018.

[114] X. Tian, T. Liu, C. Yang, Q. Wang, D. Li, Interface and performance of 3D printed continuous carbon fibre reinforced PLA composites, Compos. Appl. Sci. Manuf. 88 (2016) 198–205, https://doi.org/10.1016/j.compositesa.2016.05.032.

[115] L. Sang, S. Han, Z. Li, X. Yang, W. Hou, Development of short basalt fibre reinforced polylactide composites and their feasible evaluation for 3D printing applications, Compos. B Eng. 164 (2019) 629–639, https://doi.org/10.1016/j.compositesb.2019.01.085.

[116] J. Zhu, J. Zhang, J. Wang, B. Wang, Compatibilizer assistant SCF/ABS composites with improved mechanical properties prepared by fused deposition modeling, Polym. Plast. Technol. Eng. 57 (2018) 1576–1584, https://doi.org/10.1080/03602559.2017.1410843.

[117] M. Heidari-Rarani, M. Rafiee-Afarani, A.M. Zahedi, Mechanical characterization of FDM 3D printing of continuous carbon fibre reinforced PLA composites, Compos. B Eng. 175 (2019) 107147, https://doi.org/10.1016/j.compositesb.2019.107147.

[118] J.M. Chacón, M.A. Caminero, P.J. Núñez, E. García-Plaza, I. García-Moreno, J. M. Reverte, Additive manufacturing of continuous fibre reinforced thermoplastic composites using fused deposition modelling: effect of process parameters on mechanical properties, Compos. Sci. Technol. 181 (2019) 107688, https://doi.org/10.1016/j.compscitech.2019.107688.

[119] A.M. Forster, Materials testing standards for additive manufacturing of polymer materials: state of the art and standards applicability, 8059, https://doi.org/10.6028/NIST.IR.8059, 2015.

[120] ISO - ISO 17296-3, Additive manufacturing — general principles — Part 3: main characteristics and corresponding test methods n.d. https://www.iso.org/standard/61627.html, 2014 accessed July 5, 2020.

[121] H. Al Abadi, H.T. Thai, V. Paton-Cole, V.I. Patel, Elastic properties of 3D printed fibre-reinforced structures, Compos. Struct. 193 (2018) 8–18, https://doi.org/10.1016/j.compstruct.2018.03.051.

[122] I.V.R.W. Gray, D.G. Baird, J.H. Bøhn, Effects of processing conditions on short TLCP fibre reinforced FDM parts, Rapid Prototyp. J. 4 (1998) 14–25, https://doi.org/10.1108/13552549810197514.

[123] F. Ning, W. Cong, J. Qiu, J. Wei, S. Wang, Additive manufacturing of carbon fibre reinforced thermoplastic composites using fused deposition modeling, Compos. B Eng. 80 (2015) 369–378, https://doi.org/10.1016/j.compositesb.2015.06.013.

[124] G. Liao, Z. Li, Y. Cheng, D. Xu, D. Zhu, S. Jiang, et al., Properties of oriented carbon fibre/polyamide 12 composite parts fabricated by fused deposition modeling, Mater. Des. 139 (2018) 283–292, https://doi.org/10.1016/j.matdes.2017.11.027.

[125] Y. Li, S. Gao, R. Dong, X. Ding, X. Duan, Additive manufacturing of PLA and CF/PLA binding layer specimens via fused deposition modeling, J. Mater. Eng. Perform. 27 (2018) 492–500, https://doi.org/10.1007/s11665-017-3065-0.

[126] Ö. Keleş, E.H. Anderson, J. Huynh, Mechanical reliability of short carbon fibre reinforced ABS produced via vibration assisted fused deposition modeling, Rapid Prototyp. J. 24 (2018) 1572–1578, https://doi.org/10.1108/RPJ-12-2017-0247.

[127] M.L. Shofner, K. Lozano, F.J. Rodríguez-Macías, E.V. Barrera, Nanofibre-reinforced polymers prepared by fused deposition modeling, J. Appl. Polym. Sci. 89 (2003) 3081–3090, https://doi.org/10.1002/app.12496.

[128] K.I. Mori, T. Maeno, Y. Nakagawa, Dieless forming of carbon fibre reinforced plastic parts using 3D printer, in: Procedia Engineering, vol. 81, Elsevier Ltd, 2014, pp. 1595–1600, https://doi.org/10.1016/j.proeng.2014.10.196.

[129] A. El Magri, K. El Mabrouk, S. Vaudreuil, M. Ebn Touhami, Mechanical properties of CF-reinforced PLA parts manufactured by fused deposition modeling,

J. Thermoplast. Compos. Mater. (2019), https://doi.org/10.1177/0892705719847244, 089270571984724.
[130] R.W. Gray Iv, D.G. Baird, J.H. Bøhn, Thermoplastic composites reinforced with long fibre thermotropic liquid crystalline polymers for fused deposition modeling, Polym. Compos. 19 (1998) 383–394, https://doi.org/10.1002/pc.10112.
[131] B. Akhoundi, A.H. Behravesh, A. Bagheri Saed, Improving mechanical properties of continuous fibre-reinforced thermoplastic composites produced by FDM 3D printer, J. Reinforc. Plast. Compos. 38 (2019) 99–116, https://doi.org/10.1177/0731684418807300.
[132] R. Matsuzaki, M. Ueda, M. Namiki, T.K. Jeong, H. Asahara, K. Horiguchi, et al., Three-dimensional printing of continuous-fibre composites by in-nozzle impregnation, Sci. Rep. 6 (2016) 1–7, https://doi.org/10.1038/srep23058.
[133] W. Hao, Y. Liu, H. Zhou, H. Chen, D. Fang, Preparation and characterization of 3D printed continuous carbon fibre reinforced thermosetting composites, Polym. Test. 65 (2018) 29–34, https://doi.org/10.1016/j.polymertesting.2017.11.004.
[134] F Van Der Klift, Y. Koga, A. Todoroki, M. Ueda, Y. Hirano, R. Matsuzaki, 3D printing of continuous carbon fibre reinforced thermo-plastic (CFRTP) tensile test specimens, Open J. Compos. Mater. (2016) 18–27, https://doi.org/10.4236/ojcm.2016.61003, 06.
[135] C. Yang, X. Tian, T. Liu, Y. Cao, D. Li, 3D printing for continuous fibre reinforced thermoplastic composites: mechanism and performance, Rapid Prototyp. J. 23 (2017) 209–215, https://doi.org/10.1108/RPJ-08-2015-0098.
[136] F. Ning, W. Cong, J. Wei, S. Wang, M. Zhang, Additive Manufacturing of CFRP Composites Using Fused Deposition Modeling: Effects of Carbon Fibre Content and Length, ASME International, 2015, https://doi.org/10.1115/msec2015-9436.
[137] X. Tian, T. Liu, Q. Wang, A. Dilmurat, D. Li, G. Ziegmann, Recycling and remanufacturing of 3D printed continuous carbon fibre reinforced PLA composites, J. Clean. Prod. 142 (2017) 1609–1618, https://doi.org/10.1016/j.jclepro.2016.11.139.
[138] Stoof D K.L. Milosevi, Pickering. Characterizing the mechanical properties of fused deposition modelling natural fibre recycled polypropylene composites, J. Compos. Sci. 1 (2017) 7, https://doi.org/10.3390/jcs1010007.
[139] W. Wu, P. Geng, G. Li, D. Zhao, H. Zhang, J. Zhao, Influence of layer thickness and raster angle on the mechanical properties of 3D-printed PEEK and a comparative mechanical study between PEEK and ABS, Materials 8 (2015) 5834–5846, https://doi.org/10.3390/ma8095271.
[140] L. Pyl, K.A. Kalteremidou, D. Van Hemelrijck, Exploration of the design freedom of 3D printed continuous fibre-reinforced polymers in open-hole tensile strength tests, Compos. Sci. Technol. 171 (2019) 135–151, https://doi.org/10.1016/j.compscitech.2018.12.021.
[141] G. Dong, Y. Tang, D. Li, Y.F. Zhao, Mechanical properties of continuous kevlar fibre reinforced composites fabricated by fused deposition modeling process, in: Procedia Manufacturing, vol. 26, Elsevier B.V., 2018, pp. 774–781, https://doi.org/10.1016/j.promfg.2018.07.090.
[142] D. Stoof, K. Pickering, Y. Zhang, Fused deposition modelling of natural fibre/polylactic acid composites, J. Compos. Sci. 1 (2017) 8, https://doi.org/10.3390/jcs1010008.
[143] A. Le Duigou, A. Barbé, E. Guillou, M. Castro, 3D printing of continuous flax fibre reinforced biocomposites for structural applications, Mater. Des. 180 (2019) 107884, https://doi.org/10.1016/j.matdes.2019.107884.
[144] C. Oztan, R. Karkkainen, M. Fittipaldi, G. Nygren, L. Roberson, M. Lane, et al., Microstructure and mechanical properties of three dimensional-printed continuous fibre composites, J. Compos. Mater. 53 (2019) 271–280, https://doi.org/10.1177/0021998318781938.
[145] V.C. Gavali, P.R. Kubade, H.B. Kulkarni, Property enhancement of carbon fibre reinforced polymer composites prepared by fused deposition modeling, Mater. Today: Proceedings 23 (2020) 221–229, https://doi.org/10.1016/j.matpr.2020.02.020.
[146] G.D. Goh, V. Dikshit, A.P. Nagalingam, G.L. Goh, S. Agarwala, S.L. Sing, et al., Characterization of mechanical properties and fracture mode of additively manufactured carbon fibre and glass fibre reinforced thermoplastics, Mater. Des. 137 (2018) 79–89, https://doi.org/10.1016/j.matdes.2017.10.021.
[147] Q. Hu, Y. Duan, H. Zhang, D. Liu, B. Yan, F. Peng, Manufacturing and 3D printing of continuous carbon fibre prepreg filament, J. Mater. Sci. 53 (2018) 1887–1898, https://doi.org/10.1007/s10853-017-1624-2.
[148] M.A. Caminero, J.M. Chacón, I. García-Moreno, G.P. Rodríguez, Impact damage resistance of 3D printed continuous fibre reinforced thermoplastic composites using fused deposition modelling, Compos. B Eng. 148 (2018) 93–103, https://doi.org/10.1016/j.compositesb.2018.04.054.
[149] F. Daver, K.P.M. Lee, M. Brandt, R. Shanks, Cork–PLA composite filaments for fused deposition modelling, Compos. Sci. Technol. 168 (2018) 230–237, https://doi.org/10.1016/j.compscitech.2018.10.008.
[150] P. Wang, B. Zou, S. Ding, C. Huang, Z. Shi, Y. Ma, et al., Preparation of short CF/GF reinforced PEEK composite filaments and their comprehensive properties evaluation for FDM-3D printing, Compos. B Eng. 198 (2020) 108175, https://doi.org/10.1016/j.compositesb.2020.108175.
[151] J. Nagendra, M.S.G. Prasad, FDM process parameter optimization by taguchi technique for augmenting the mechanical properties of nylon–aramid composite used as filament, Material. J. Ins. Eng. (India): Series C 101 (2020) 313–322, https://doi.org/10.1007/s40032-019-00538-6.
[152] R. Guo, Z. Ren, H. Bi, Y. Song, M. Xu, Effect of toughening agents on the properties of poplar wood flour/poly (lactic acid) composites fabricated with Fused Deposition Modeling, Eur. Polym. J. 107 (2018) 34–45, https://doi.org/10.1016/j.eurpolymj.2018.07.035.
[153] V.C. Gavali, P.R. Kubade, H.B. Kulkarni, Mechanical and thermo-mechanical properties of carbon fibre reinforced thermoplastic composite fabricated using fused deposition modeling method, in: Materials Today: Proceedings, vol. 22, Elsevier Ltd, 2019, pp. 1786–1795, https://doi.org/10.1016/j.matpr.2020.03.012.
[154] V. Dikshit, Y.L. Yap, G.D. Goh, H. Yang, J.C. Lim, X. Qi, et al., Investigation of out of plane compressive strength of 3D printed sandwich composites, IOP Conf. Ser. Mater. Sci. Eng. 139 (2013), https://doi.org/10.1088/1757-899X/139/1/012017, 012017.
[155] Z. Hou, X. Tian, J. Zhang, D. Li, 3D printed continuous fibre reinforced composite corrugated structure, Compos. Struct. 184 (2018) 1005–1010, https://doi.org/10.1016/j.compstruct.2017.10.080.
[156] M. Kaur, T.G. Yun, S.M. Han, E.L. Thomas, W.S. Kim, 3D printed stretching-dominated micro-trusses, Mater. Des. 134 (2017) 272–280, https://doi.org/10.1016/j.matdes.2017.08.061.
[157] A.K. Sood, R.K. Ohdar, S.S. Mahapatra, Experimental investigation and empirical modelling of FDM process for compressive strength improvement, J. Adv. Res. 3 (2012) 81–90, https://doi.org/10.1016/j.jare.2011.05.001.
[158] M. Araya-Calvo, I. López-Gómez, N. Chamberlain-Simon, J.L. León-Salazar, T. Guillén-Girón, J.S. Corrales-Cordero, et al., Evaluation of compressive and flexural properties of continuous fibre fabrication additive manufacturing technology, Additive Manufac. 22 (2018) 157–164, https://doi.org/10.1016/j.addma.2018.05.007.
[159] X. Han, D. Yang, C. Yang, S. Spintzyk, L. Scheideler, P. Li, et al., Carbon fibre reinforced PEEK composites based on 3D-printing technology for orthopedic and dental applications, J. Clin. Med. 8 (2019) 240, https://doi.org/10.3390/jcm8020240.
[160] S. Kain, J.V. Ecker, A. Haider, M. Musso, A. Petutschnigg, Effects of the infill pattern on mechanical properties of fused layer modeling (FLM) 3D printed wood/polylactic acid (PLA) composites, Europ. J. Wood Wood Prod. 78 (2020) 65–74, https://doi.org/10.1007/s00107-019-01473-0.
[161] T.-C. Yang, Effect of extrusion temperature on the physico-mechanical properties of unidirectional wood fibre-reinforced polylactic acid composite (WFRPC) components using fused deposition modeling, Polymers 10 (2018) 976, https://doi.org/10.3390/polym10090976.
[162] E. Verdejo de Toro, J. Coello Sobrino, A. Martínez Martínez, V. Miguel Eguía, J. Ayllón Pérez, Investigation of a short carbon fibre-reinforced polyamide and comparison of two manufacturing processes: fused deposition modelling (FDM) and polymer injection moulding (PIM), Materials 13 (2020) 672, https://doi.org/10.3390/ma13030672.
[163] W. Zhang, A.S. Wu, J. Sun, Z. Quan, B. Gu, B. Sun, et al., Characterization of residual stress and deformation in additively manufactured ABS polymer and composite specimens, Compos. Sci. Technol. 150 (2017) 102–110, https://doi.org/10.1016/j.compscitech.2017.07.017.
[164] Stepashkin, D.I. Chukov, F.S. Senatov, A.I. Salimon, A.M. Korsunsky, S. D. Kaloshkin, 3D-printed PEEK-carbon fibre (CF) composites: structure and thermal properties, Compos. Sci. Technol. 164 (2018) 319–326, https://doi.org/10.1016/j.compscitech.2018.05.032.
[165] E.V. De Toro, J.C. Sobrino, A.M. Martínez, V.M. Eguía, Analysis of the influence of the variables of the fused deposition modeling (FDM) process on the mechanical properties of a carbon fibre-reinforced polyamide, in: Procedia Manufacturing, vol. 41, Elsevier B.V., 2019, pp. 731–738, https://doi.org/10.1016/j.promfg.2019.09.064.
[166] M. Vinyas, S.J. Athul, D. Harursampath, T. Nguyen Thoi, Experimental evaluation of the mechanical and thermal properties of 3D printed PLA and its composites, Mater. Res. Express 6 (2019) 115301, https://doi.org/10.1088/2053-1591/ab43ab.